Preprints.org

Article

Not peer-reviewed version

Multi-Omics Insights into the Effects of Probiotics and Vitamin D on Clinical Signature, Inflammation, Metabolism, and Microbiota in Oral Lichen Planus: The MICROCOSM In Vivo Study

Paola Zanetta , Matteo Calgaro , Marta Mellai , Alessia Vignoli , Monica Marotta , Nicola Vitulo , Leonardo Tenori , Marcello Manfredi , Elettra Barberis , Mario Migliario , Marta Armari , Valeria Caneparo , Diletta Francesca Squarzanti , Marta Allesina , Angela Amoruso , Marco Pane , Barbara Azzimonti *

Posted Date: 22 May 2026

doi: 10.20944/preprints202605.1565.v1

Keywords: Oral Lichen Planus (OLP); oral squamous cell carcinoma (OSCC); oral and gut microbiota; vitamin D; probiotics (*Limosilactobacillus reuteri; Lacticasebacillus rhamnosus; and Lacticasebacillus casei*); proinflammatory cytokines; metabolomics; proteomics; 16S RNA sequencing

Preprints.org is a free multidisciplinary platform providing preprint service that is dedicated to making early versions of research outputs permanently available and citable. Preprints posted at Preprints.org appear in Web of Science, Crossref, Google Scholar, Scilit, Europe PMC, OpenAlex.

Copyright: This open access article is published under a Creative Commons CC BY 4.0 license, which permit the free download, distribution, and reuse, provided that the author and preprint are cited in any reuse.

Preprints.org (www.preprints.org) | NOT PEER-REVIEWED | Posted: 22 May 2026 doi:10.20944/preprints202605.1565.v1

Disclaimer/Publisher's Note: The statements, opinions, and data contained in all publications are solely those of the individual author(s) and contributor(s) and not of MDPI and/or the editor(s). MDPI and/or the editor(s) disclaim responsibility for any injury to people or property resulting from any ideas, methods, instructions, or products referred to in the content.

Article

Multi-Omics Insights into the Effects of Probiotics and Vitamin D on Clinical Signature, Inflammation, Metabolism, and Microbiota in Oral Lichen Planus: the MICROCOSM In Vivo Study

Paola Zanetta [1,†], Matteo Calgaro [2,†], Marta Mellai [3], Alessia Vignoli [4,5], Monica Marotta [6], Nicola Vitulo [2], Leonardo Tenori [4,5], Marcello Manfredi [7], Elettra Barberis [8], Mario Migliario [6,9], Marta Armari [1], Valeria Caneparo [10], Diletta Francesca Squarzanti [1], Marta Allesina [3], Angela Amoruso [11], Marco Pane [11] and Barbara Azzimonti [1,*]

1 Laboratory of Applied Microbiology, Center for Translational Research on Allergic and Autoimmune Diseases (CAAD), Department of Health Sciences (DiSS), School of Medicine, Università del Piemonte Orientale (UPO), Corso Trieste 15/A, 28100 Novara, Italy
2 Department of Biotechnology, University of Verona, Strada le Grazie, 15, 37134 Verona, Italy
3 Integrative Genomics Core Facility, Center for Translational Research on Allergic and Autoimmune Diseases (CAAD), Department of Health Sciences (DiSS), School of Medicine, Università del Piemonte Orientale (UPO), Corso Trieste 15/A, 28100 Novara, Italy
4 Department of Chemistry "Ugo Schiff", University of Florence, Via della Lastruccia 3-13, 50019 Sesto Fiorentino, Italy
5 Magnetic Resonance Center (CERM), University of Florence, Via Luigi Sacconi 6, Sesto Fiorentino, 50019 Firenze, Italy;
6 Odontostomatology Unit, Azienda Ospedaliero Universitaria (AOU) "Maggiore della Carita", 28100 Novara, Italy
7 Biological Mass Spectrometry, Center for Translational Research on Allergic and Autoimmune Diseases (CAAD), Department of Translational Medicine (DiMeT), School of Medicine, Università del Piemonte Orientale (UPO), Corso Trieste 15/A, 28100 Novara, Italy
8 Center for Translational Research on Allergic and Autoimmune Diseases (CAAD), Department of Sciences and Technological Innovation, University of Piemonte Orientale, 15121 Alessandria, Italy
9 Department of Translational Medicine, School of Medicine, Università del Piemonte orientale (UPO), 28100 Novara, Italy
10 Protein Technologies Core Facility, Center for Translational Research on Allergic and Autoimmune Diseases (CAAD), Department of Translational Medicine, School of Medicine, Università del Piemonte Orientale (UPO), Corso Trieste 15/A, 28100 Novara, Italy
11 Probiotical Research S.R.L, Via Mattei 3, 28100, Novara, Italy
* Correspondence: barbara.azzimonti@uniupo.it
† These authors contributed equally to this work.

Abstract

Oral lichen planus (OLP) is a chronic inflammatory oral disease associated with immune dysregulation and malignant transformation risk. Vitamin D and probiotics may modulate immune and microbial pathways involved in OLP. In this study, we evaluated their effects on clinical outcomes and multi-omics profiles in 25 adult OLP patients. Vitamin D-deficient patients received 2,000 IU/day vitamin D3, and all participants received a probiotic blend (*Limosilactobacillus reuteri* LRE11, *Lacticaseibacillus rhamnosus* LR04, and *Lacticaseibacillus casei* LC04) for 16 weeks. Clinical assessments and analyses of saliva, serum, oral swabs, and stool samples were performed before and after treatment. Following the intervention, 76% of participants achieved clinical remission. Significant metabolomic changes were observed mainly in saliva and feces. Serum cytokines, metabolites, and lipoproteins showed no significant differences. Microbiome profiling demonstrated treatment-related compositional shifts in oral and fecal samples, including increased *Lacticaseibacillus* abundance. Multi-omics integration identified coordinated interactions among

© 2026 by the author(s). Distributed under a Creative Commons CC BY license.

Preprints.org (www.preprints.org) | NOT PEER-REVIEWED | Posted: 22 May 2026 doi:10.20944/preprints202605.1565.v1

microbial, metabolic, immune, and lipid pathways, highlighting interconnected gut-oral biological responses. Combined vitamin D and probiotic supplementation was associated with clinical improvement and coordinated oral-intestinal multi-omics changes, supporting a systems-level understanding of OLP remission. These findings suggest that modulating the microbiota-metabolism-immunity axis could represent a promising therapeutic strategy for achieving sustained disease control and clinical remission.

Keywords: Oral Lichen Planus (OLP); oral squamous cell carcinoma (OSCC); oral and gut microbiota; vitamin D; probiotics (*Limosilactobacillus reuteri*; *Lacticasebacillus rhamnosus*; and *Lacticasebacillus casei)*; proinflammatory cytokines; metabolomics; proteomics; 16S RNA sequencing

1. Introduction

Oral Lichen Planus (OLP) is a chronic, T-cell-mediated inflammatory disorder affecting the oral mucosa. It has a global prevalence of approximately 0.5-4%, with a higher occurrence in females [1]. Despite its known risks, OLP remains underdiagnosed or misdiagnosed due to the lack of standardized criteria [2–4]. Its variable clinical presentation, which may be asymptomatic or mimic other oral conditions, combined with limited awareness among patients and non-specialist healthcare providers, further complicates its recognition [5]. In classical lesions (bilateral, reticular pattern), it is possible to make a diagnosis based on the clinical appearance alone even if definitive diagnosis requires histological examination, which is not always performed because it is not invariably accepted by asymptomatic patients [6,7].

OLP onset and progression are influenced by multiple factors, including genetic predisposition, trauma, and environmental stressors, such as dietary components and chemicals. These factors can disrupt oral and gut microbiota, leading to dysbiosis. The depletion of beneficial microbial species allows opportunistic pathogens to flourish contributing to chronic inflammation and, potentially, to carcinogenesis [8–12].

A hallmark of OLP is a dense, band-like lymphocytic infiltrate at the epithelial-basal membrane interface, resulting in basal cell degeneration and epithelial destruction [13]. The immune response involves macrophages, monocytes, CD4+ and CD8+ T cells, dendritic cells, fibroblasts, and epithelial cells, which together drive cytokine overproduction, nuclear factor-kappa B (NF-κB) signaling activation and basal epithelial cells apoptosis. Matrix metalloproteinases (MMPs) and mast cell degranulation further sustain inflammation and tissue damage [14,15].

Clinically, OLP manifests in six forms (*i.e.*, reticular, atrophic, papular, bullous, plaque-like, and erosive-ulcerative), which may coexist in the same patient, and may involve extraoral sites, significantly impacting the patient's life quality [13,16]. Although its malignant potential was discovered over a century ago, the World Health Organization (WHO) only officially acknowledged the risk in 2005, with an estimated transformation to oral squamous cell carcinoma (OSCC) of 0.44-5%, with higher incidence in erosive/ulcerative forms, tongue lesions, female sex, and 6-7th decade of life, but none of these have achieved significant agreement among researchers [17–20].

Current OLP treatments (corticosteroids, retinoids, and immunosuppressants such as tacrolimus) primarily aim to control inflammation and symptoms. However, concerns regarding their long-term safety and variable efficacy have prompted the search for alternative solutions [21–23].

Recent research highlights the role of gut microbiota dysbiosis in OLP, particularly its impact on regulatory T cells (Treg) function [24]. This has spurred interest in probiotics as a potential adjunctive therapy. Specific strains, such as *Lacticaseibacillus rhamnosus, Lactobacillus delbrueckii, Lactobacillus johnsonii, Lactobacillus plantarum,* and *Bifidobacterium animalis*, exhibit immunomodulatory properties, influencing the Treg/T-helper 17 (Th17) axis, suppressing excessive immune responses, and promoting immune homeostasis [25–27]. Probiotics can also modulate inflammatory cytokines, such as interleukin (IL)-10 and transforming growth factor-beta (TGF-β), thereby mitigating chronic OLP-associated inflammation. Evidence from our group demonstrated that probiotic Cell Free

© 2026 by the author(s). Distributed under a Creative Commons CC BY license.

Preprints.org (www.preprints.org) | NOT PEER-REVIEWED | Posted: 22 May 2026 doi:10.20944/preprints202605.1565.v1

Supernatants (CFSs), together with vitamin D, reduce IL-6 production and counteract cytotoxicity in oral epithelial cells exposed to periodontal pathogens [28].

In addition, other studies on other immune-mediated diseases such as rheumatoid arthritis [29] and experimental autoimmune encephalomyelitis [30] suggest that probiotics enhance Treg differentiation, modulate cytokine profiles, and inhibit NF-κB signaling, providing a rationale for their application in OLP.

Vitamin D, a known immunomodulator, can suppress pro-inflammatory T-helper 1 (Th1)/Th17 responses, while enhancing regulatory cytokines [31]. Since vitamin D deficiency has been frequently reported in OLP and has been associated with higher disease activity, correcting low vitamin D status may contribute to symptom/lesion improvement and to the modulation of inflammatory readouts, including interferon-gamma (IFN-γ) [32].

Based on these premises, probiotics and vitamin D supplementation may act as complementary immuno-microbiome modulators, potentially promoting mucosal immune homeostasis and microbial compositional shifts, while systemic effects remain to be clarified [33,34]. Despite promising preliminary evidence, several uncertainties continue to limit the clinical application of probiotics in OLP management. These include the unknown precise mechanisms of immune modulation, the identification of optimal strains, appropriate dosage regimen and delivery methods, variability in therapeutic response across OLP subtypes, potential interactions with conventional treatments, absence of validated predictive biomarkers, and limited long-term safety data.

This pilot monocentric study investigates the impact of a 16-week intervention combining vitamin D correction (according to baseline status) and a multi-strain probiotic supplementation on clinical outcomes and multi-layer profiling in 25 OLP patients, encompassing saliva and serum cytokines, serum lipoprotein measures, metabolomics profiles (saliva, serum, and stool), and 16S rRNA-based microbiome data (saliva, stool, and lesional/non-lesional oral sites).

We aim to determine whether the intervention can improve clinical symptoms, modulate inflammatory responses, induce metabolic adaptations, and reshape microbial community composition. Findings from this study will inform larger trials to validate these effects, elucidate mechanisms of vitamin D- and probiotic-mediated immune regulation, and support the development of microbiota-based strategies for personalized OLP management.

2. Results

This section may be divided by subheadings. It should provide a concise and precise description of the experimental results, their interpretation, as well as the experimental conclusions that can be drawn.

2.1. OLP Patients' Population

A total of 25 patients were enrolled, of whom 68% were female. The median age was 68 years (IQR: 58-73). The median BMI was 24.0 kg/m² (IQR: 22.5-29.1), with 60% of participants classified as normal weight, 20% as overweight, and 20% as obese (**Table 1**).

Table 1. Demographic characteristics of OLP patients at enrolment (PRE).

Characteristic	N = 25[1]
Sex	
Female	17 (68%)
Male	8 (32%)
Age, years	68 (58, 73)
BMI, kg/m²	24.0 (22.5, 29.1)
Normal weight	15 (60%)
Overweight	5 (20%)
Disease severity	
Mild	9 (36%)

© 2026 by the author(s). Distributed under a Creative Commons CC BY license.

Preprints.org (www.preprints.org) | NOT PEER-REVIEWED | Posted: 22 May 2026 doi:10.20944/preprints202605.1565.v1

Mild-Severe	5 (20%)
Severe	11 (44%)

[1] n (%); Median (first quartile, third quartile).

OLP clinical diagnosis was based on objective examination only in 44% of the patients, while the remaining 56% had biopsy confirmation.

Patients were classified at baseline according to disease severity based on lesion type: 36% mild (reticular lesions only), 20% mild-severe (papular/plaque-like or atrophic lesions without erosive/ulcerative lesions), and 44% severe (erosive/ulcerative lesions). Representative lesion-type images are provided in **Supplementary File S1, Figure S1**.

Lesion distribution across oral sites and clinical patterns in the cohort is summarized in **Supplementary File S1, Table S1**. Cheek involvement was universal, with reticular lesions representing the predominant pattern (20/25, 80%), while papular/plaque-like (3/25, 12%) and erosive (2/25, 4%) were uncommon. Tongue involvement was less frequent, as 17/25 (68%) showed no tongue lesions; when present, tongue lesions were heterogeneous and mainly atrophic (3/25, 12%), with reticular and papular/plaque-like patterns each observed in 2/25 (8%) and erosive lesions in 1/25 (4%). Gingival lesions were observed in just over half of patients (13/25, 52%) and were largely erosive (11/25, 44%, *i.e.*, the 100% of severe cases), whereas papular/plaque-like gingival lesions were rare (2/25, 8%).

Comorbidities and ongoing systemic therapies were collected as part of baseline cohort characterization (**Supplementary File S1, Tables S2–S5**). Potentially OLP-related comorbidities and other comorbidities are summarized in **Supplementary File S1, Tables S2 and S3**, respectively. Systemic medications potentially associated with OLP and medications potentially decreasing salivary flow are reported in **Supplementary File S1, Tables S4 and S5**.

2.2. Vitamin D Supplementation

A summary of vitamin D supplementation types and serum concentrations at the baseline is presented in **Supplementary File S1, Table S6**. Vitamin D supplementation wasn't required in 10 patients as their baseline levels were within the normal range (20-40 ng/mL) according to the Italian Drug Agency (Agenzia Italiana del Farmaco, AIFA). Of the remaining patients, 8 were already receiving pharmacological supplementation (Dibase, Didrogyl), while 7 started vitamin D supplementation at PRE.

Vitamin D levels in patients' sera were also measured at POST. Overall, a significant increase (p=0.03) was observed from PRE to POST (**Supplementary File S1, Figure S2a**). More specifically, patients who had vitamin D levels within the normal range at PRE, whether chronically supplementing or not, showed an almost stable trend over time (**Supplementary File S1, Figure S2b**). In contrast, those who started vitamin D supplementation for the first time at enrollment exhibited a significant increase in 25[OH]D levels (p<0.01).

2.3. Clinical Response

Lesion characteristics improved from baseline to post-intervention (**Figure 1**). Lesion number showed a statistically significant change (p<0.001), with most patients shifting toward lower lesion-count (52%, **Figure 1a**). Largest lesion size also changed significantly (p=0.004), with an overall redistribution toward smaller size categories (**Figure 1b**). Bleeding activity improved (p=0.014), with a higher proportion of patients showing no bleeding lesions at POST (52% vs 84%, **Figure 1c**). To integrate changes across lesion number, largest lesion size, and bleeding lesions, a composite Clinical Activity Index was derived by assigning each marker a score (−1 remission, 0 stability, +1 recurrence) and summing scores across markers; 19 patients were classified as overall remission (76%), with 4 remaining stable (16%), and only 2 showing recurrence (8%). The distribution was strongly skewed toward remission (p<0.001; **Figure 1d**).

© 2026 by the author(s). Distributed under a Creative Commons CC BY license.

Preprints.org (www.preprints.org) | NOT PEER-REVIEWED | Posted: 22 May 2026 doi:10.20944/preprints202605.1565.v1

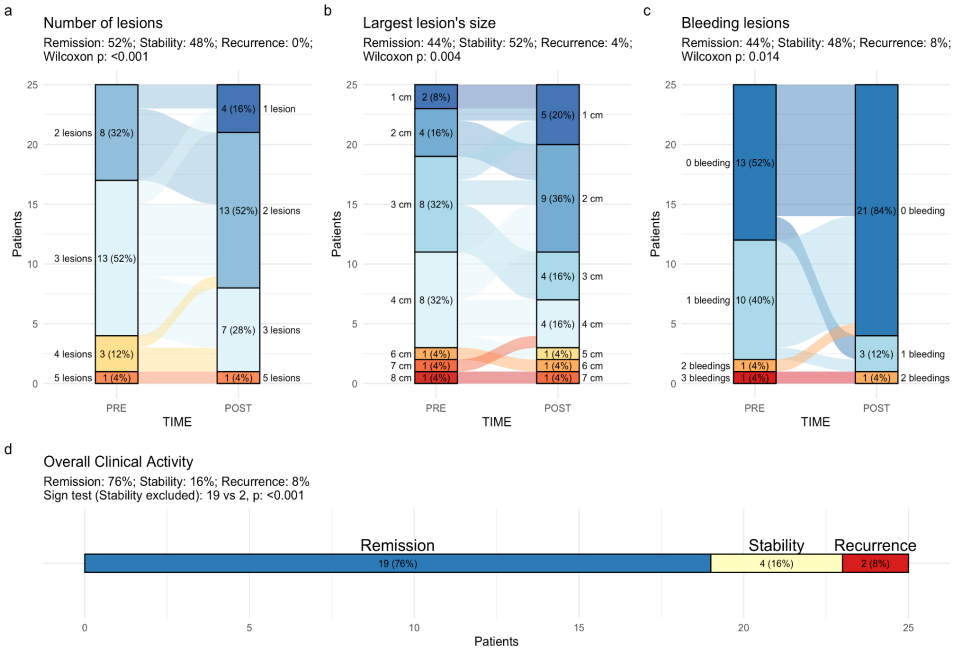

Figure 1. Individual changes in lesion-related outcomes and overall clinical activity after the 16-week intervention period. Panels (**a-c**) display patient-level transitions from baseline (PRE) to post-treatment (POST) for (**a**) lesion number, (**b**) largest lesion size (cm), and (**c**) number of bleeding lesions, with strata indicating the distribution across categories at each time point. Paired PRE-POST differences were assessed using the Wilcoxon signed-rank test. Panel (**d**) shows the composite Clinical Activity classification (see Materials and Methods). The directional imbalance toward remission was evaluated using a sign test excluding stable cases.

2.4. Inflammatory Profile

To explore whether the intervention was associated with immune modulation, we evaluated time-related changes across a panel of salivary and serum cytokines. After multiple-testing correction, no cytokine met the significance threshold (p=0.05); nevertheless, the largest percentage reductions were observed for salivary IL-21 (42%) and IL-33 (61%), with a small decrease in serum TGF-β2 (4%) (**Supplementary File S1, Tables S7-S8**).

2.5. Serum Metabolomics and Lipoproteomics Analyses

Following the cytokine analyses, we next assessed whether the intervention was associated with broader systemic biochemical changes by examining the serum NMR metabolomics and lipoprotein profiles.

After FDR correction, no serum metabolite or lipoprotein feature reached statistical significance. Descriptively, the most notable absolute changes were an increase in alanine and shifts in lipoprotein measures, including higher phospholipids in VLDL1 and higher triglycerides in IDL and VLDL1, alongside lower triglycerides in LDL and LDL1 (**Supplementary File S1, Tables S9–S10**).

2.6. Salivary and Fecal Metabolomics Analyses

We then extended profiling to untargeted GC×GC–MS metabolomics in saliva and feces to capture local and intestinal metabolic readouts potentially accompanying the intervention.

Untargeted metabolomics analysis detected and quantified 330 salivary and 255 fecal metabolites. After multiple testing corrections, 85 salivary metabolites (16 increased, 69 decreased; **Supplementary File S1, Table S11**) and 34 fecal metabolites (19 increased, 15 decreased; **Supplementary File S1, Table S12**), changed significantly (p<0.05).

© 2026 by the author(s). Distributed under a Creative Commons CC BY license.

Preprints.org (www.preprints.org) | NOT PEER-REVIEWED | Posted: 22 May 2026 doi:10.20944/preprints202605.1565.v1

In saliva, significant changes included decreases in L-threonine and other amino acids (e.g., L-leucine, L-valine), together with decreases in carbohydrate-related features (β-D-(+)-xylopyranose, D-arabinose, D-mannose, ribitol, 1,5-anhydroglucitol) and in tryptophan-related metabolites (indoleacetic acid and anthranilic acid) (**Supplementary File S1, Table S11**). Lipid-related features changed in both directions, with decreases in hexadecanamide, octadecanamide, and palmitic acid and increases in several fatty acids (including myristic acid), while the strongest increases included malonic acid, diglycerol, xylitol, L-aspartic acid, and hippuric acid (**Supplementary File S1, Table S11**).

In feces, significant changes included decreases in pimelic acid, glycine, D-(-)-fructofuranose, and 3-hydroxybutyric acid (β-hydroxybutyrate), alongside increases in methyl α-D-glucofuranoside, catechol, 1-monooleoylglycerol, xylonic acid, erythritol, niacinamide, adenine, and the dipeptide Ser–Leu (**Supplementary File S1, Table S12**).

Pathway analysis highlighted valine, leucine and isoleucine biosynthesis and alanine, aspartate and glutamate metabolism in saliva (**Figure 2a**), and glycine, serine and threonine metabolism together with alanine, aspartate and glutamate metabolism in feces (**Figure 2b**).

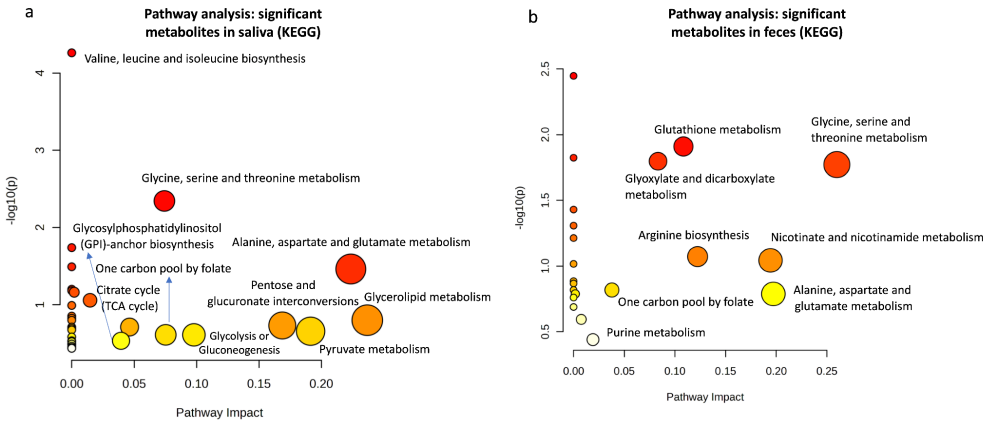

Figure 2. KEGG pathway impact plots of significantly changed metabolites in saliva (**a**) and feces (**b**) following the 16-week intervention. Pathways were identified using over-representation analysis with pathway topology impact. The y-axis shows enrichment significance (-log10 *p*-value), and the x-axis shows pathway impact from topology analysis; larger and darker bubbles indicate pathways with greater impact and significance. Selected pathways with the highest impact and/or significance are labeled in each panel.

2.7. 16S Metabarcording

To complement the immune and metabolomics layers, we next profiled the oral and gut microbiome using 16S rRNA gene metabarcoding across S, L, NL, and F samples, focusing on community structure (α/β-diversity) and genus-level differential abundance between time points.

2.7.1. Samples Quality and Microbial Composition

Sequencing generated high-quality 16S rRNA gene data across all sample types (S, L, NL, and F; **Supplementary File S1, Table S13**). All samples exceed 20.000 high-quality reads. Rarefaction curves (**Supplementary File S1, Figure S3**) approached saturation, indicating that microbial richness was adequately captured in all samples.

After genus-level agglomeration and prevalence filtering, we obtained an average of ~120 microbial features in oral cavity specimens (S, L, and NL) and ~160 features in stool samples (F; **Supplementary File S1, Table S14**). Relative-abundance profiles (Figure 3) showed that the microbial community was overall dominated by members of the Bacillota phylum across all specimen types, with Actinomycetota also contributing substantially. In stool, Bacteroidota represented an additional major component of the community. At the genus level, the dataset encompassed most of the genera

© 2026 by the author(s). Distributed under a Creative Commons CC BY license.

Preprints.org (www.preprints.org) | NOT PEER-REVIEWED | Posted: 22 May 2026 doi:10.20944/preprints202605.1565.v1

belonging to Bacillota, Pseudomonadota, Actinomycetota, and Bacteroidota, while fewer than ten genera were detected for each of the remaining phyla represented in the dataset (see **Supplementary File S1, Tables S15-S16** for more details).

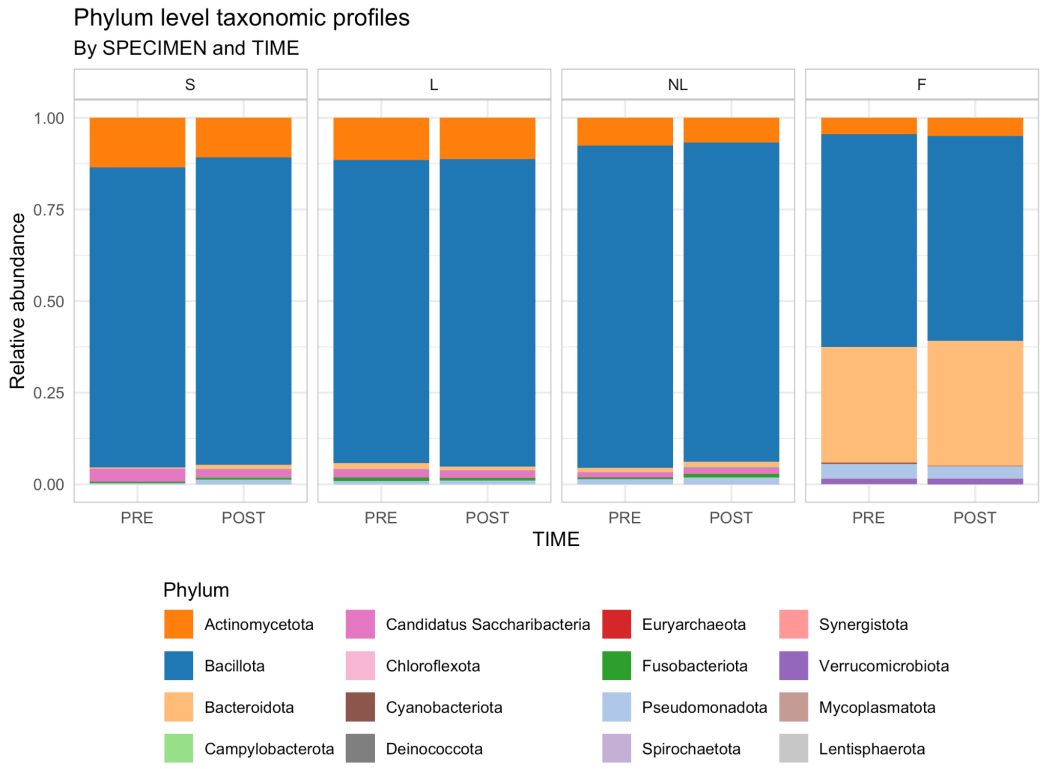

Figure 3. Phylum-level average relative abundance profiles in saliva (S), OLP-lesional mucosa (L), non-lesional mucosa (NL), and feces (F) specimens before (PRE) and after the 16-week intervention period (POST).

2.7.2. Ecological Analyses

α-diversity metrics showed marked differences between specimen types, whereas no relevant changes were observed over time (**Figure 4**). Stool samples displayed substantially higher richness and Shannon diversity than all oral cavity specimens (S, L, and NL), with consistently significant contrasts across all metrics (**Supplementary File S1, Table S17**). Oral samples, by contrast, exhibited lower richness and a more uneven taxonomic structure, largely driven by the dominance of a single genus, *Streptococcus*, which accounted on average for approximately 38% of total counts. Relative dominance was therefore significantly higher in oral specimens compared with fecal samples.

Across all specimen types, PRE–POST contrasts showed no significant differences after the 16-week intervention, indicating that α-diversity remained stable over time.

© 2026 by the author(s). Distributed under a Creative Commons CC BY license.

Preprints.org (www.preprints.org) | NOT PEER-REVIEWED | Posted: 22 May 2026 doi:10.20944/preprints202605.1565.v1

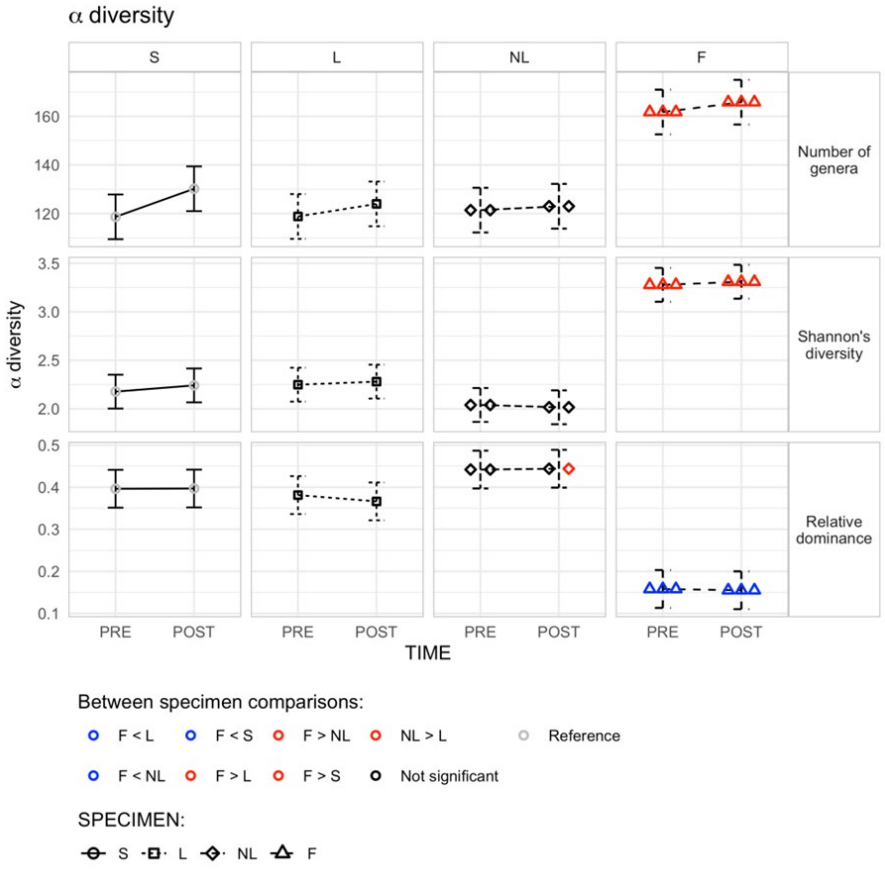

Figure 4. Adjusted α-diversity metrics (number of genera, relative dominance of the most abundant genus, and Shannon diversity index) before (PRE) and after (POST) the 16-week intervention, stratified by specimen type: saliva (S), OLP-lesional mucosa (L), non-lesional mucosa (NL), and feces (F). Values represent model-estimated means (and 95% CI) obtained from linear mixed-effects models adjusted for baseline covariates (age, sex, BMI, baseline Vitamin D concentration, and disease severity). Outline colours mark significant differences across specimens (S vs L, S vs NL, L vs NL, S vs F, L vs F, NL vs F) at a given time point. Asterisks indicate significant changes across time points, within each specimen (none are present).

β-diversity analyses revealed clear global differences in microbial community composition across specimen types. PERMANOVA confirmed that body site accounted for a substantial proportion of overall variability (51.18%, $p<0.01$), with significant between-specimen dissimilarities and heterogeneous dispersion patterns, particularly lower dispersion in fecal samples ($p<0.01$, **Figure 5a**). When analysing each body site separately, a significant global effect of the treatment period was detected ($p<0.01$ in S, L, F, and $p=0.02$ in NL), indicating that the intervention was associated with shifts in microbial composition across all specimen types (**Figure 5b-e**).

© 2026 by the author(s). Distributed under a Creative Commons CC BY license.

Preprints.org (www.preprints.org) | NOT PEER-REVIEWED | Posted: 22 May 2026 doi:10.20944/preprints202605.1565.v1

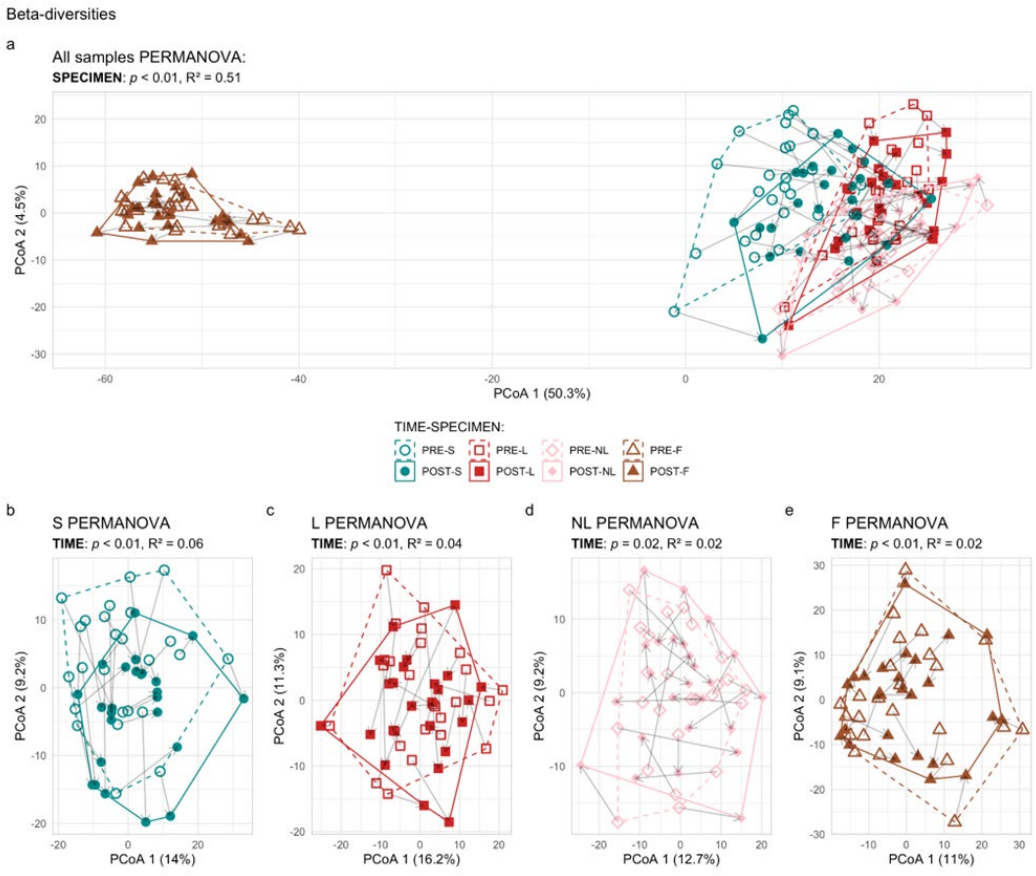

Figure 5. β-diversity based on PCoA of Aitchison distances. Saliva (S), OLP-lesional mucosa (L), non-lesional mucosa (NL), and fecal (F) samples are differentiated by colors and shapes. Empty symbols and dashed convex hulls represent baseline samples (PRE), whereas filled symbols and solid convex hulls represent samples collected after the 16-week intervention (POST). PERMANOVA results are reported in each panel's title, showing the p-value and the proportion of variability explained by the variable of interest (R^2). Panels: **a.** all specimens. **b.** saliva (S) samples. **c.** OLP-lesional mucosa (L) samples. **d.** non-lesional mucosa (NL) samples. **e.** fecal (F) samples.

2.7.3. Differential Abundance Analysis

The differential abundance analysis identified several taxa whose CLR abundances differed significantly between PRE and POST (**Figure 6**). Patterns were highly specimen-specific.

In saliva, several genera within Actinomycetota (e.g., *Lancefieldella*) and Bacillota (e.g., *Bulleidia*) phyla showed decreased abundances at POST (**Figure 6a**). In contrast, significant increases were observed for *Lacticaseibacillus* and *Schleiferilactobacillus* (Bacillota), *Cloacibacterium* (Bacteroidota), *Arcobacter* (Campylobacterota), *Pseudoleptotrichia*, *Acetobacter*, *Morococcus*, and *Neisseria* (Pseudomonadota) (**Figure 6b**). A small number of additional unclassified taxa also displayed changes in the same directions.

OLP-lesional mucosa samples showed a clear tendency toward increased abundances at POST (**Figure 6c**). Significant increases were detected in genera belonging to Bacillota, Bacteroidota, Campylobacterota, and Pseudomonadota, including *Lacticaseibacillus*, *Chryseobacterium*, *Arcobacter*, and *Acetobacter*, respectively. A few additional unclassified taxa also exhibited increases.

Non-lesional mucosa also showed exclusively increased taxa at POST (**Figure 6d**), including genera from Actinomycetota, Bacteroidota, and Fusobacteriota (e.g., *Slackia*, unclassified *Weeksellaceae*, and *Leptotrichia*), with no significant decreases detected.

Stool samples exhibited fewer changes overall (**Figure 6e-f**). Unclassified Bacteroidota sequences decreased, while two Bacillota genera, *Lacticaseibacillus* and *Limisilactobacillus*, showed increases, consistent with the composition of the administered probiotic.

© 2026 by the author(s). Distributed under a Creative Commons CC BY license.

Preprints.org (www.preprints.org) | NOT PEER-REVIEWED | Posted: 22 May 2026 doi:10.20944/preprints202605.1565.v1

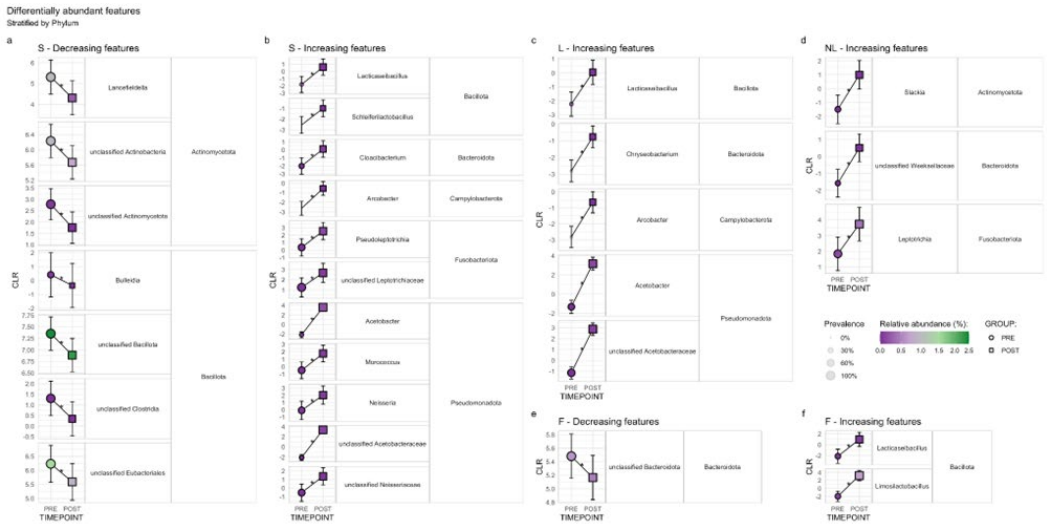

Figure 6. Differentially abundant taxa before (PRE, circle-shaped) and after (POST, square-shaped) the 16-week intervention. Values represent model-estimated means obtained from linear mixed-effects models adjusted for baseline covariates (age, sex, BMI, baseline Vitamin D concentration, and disease severity). Point size reflects prevalence across samples, and point color represents relative abundance. Asterisks indicate significant changes across time points. **a**. Saliva (S) decreased taxa. **b**. Saliva (S) increased taxa. **c**. OLP-lesional mucosa (L) increased taxa. **d**. Non-lesional mucosa (NL) increased taxa. **e**. Feces (F) decreased taxon. **f**. Feces (F) increased taxa.

2.8. Multi-Omics Integration

To identify coordinated time-related changes shared across molecular layers, we applied MOFA to covariate-adjusted within-subject deltas (POST-PRE) from cytokines, metabolomics, serum lipoproteins, and microbiome profiles.

The final model retained three latent factors, summarizing the major axes of cross-omics covariation.

2.8.1. Variance Explained Across Omics Layers

Across the model, salivary metabolomics showed the largest cumulative fraction of variance explained (26.56%), followed by 16S-L (12.95%), MET-F (11.87%), CYT-S (11.77%), and LIP-Se (9.03%). Smaller contributions were observed for 16S-NL (8.95%), 16S-F (8.68%), 16S-S (7.99%), and CYT-Se (2.62%), while MET-Se contributed negligibly (**Figure 7a**).

When stratified by factor, Factor 1 displayed broad multi-view contributions (notably lipoproteins and several microbiome compartments), Factor 2 was predominantly characterized by metabolomics, and Factor 3 by salivary metabolomics and salivary cytokines (**Figure 7b**).

To facilitate interpretation, each factor was examined individually by considering view-level variance contributions and top-weighted features ($|weight|>0.1$).

© 2026 by the author(s). Distributed under a Creative Commons CC BY license.

Preprints.org (www.preprints.org) | NOT PEER-REVIEWED | Posted: 22 May 2026 doi:10.20944/preprints202605.1565.v1

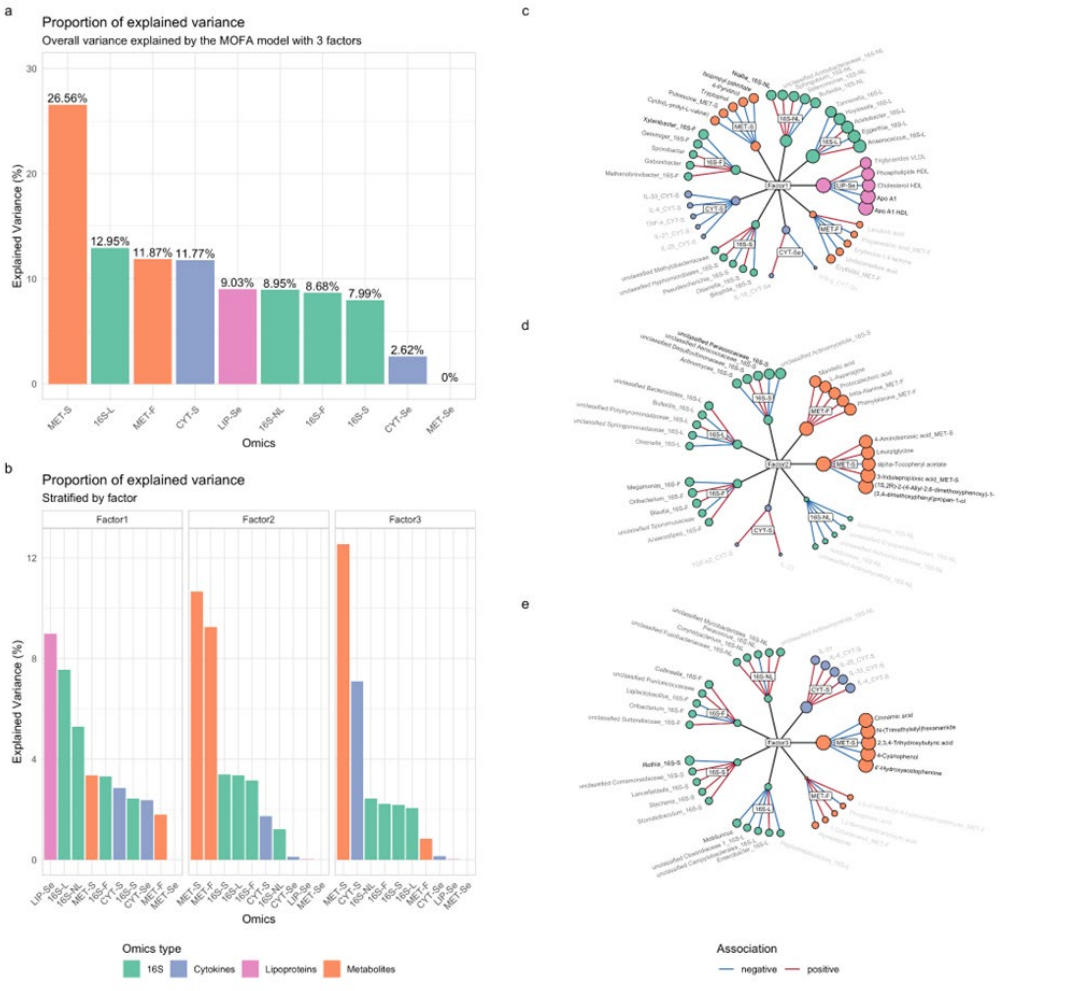

Figure 7. Multi-omics integration and latent factor structure identified by MOFA. The MOFA model integrates microbiome profiles from saliva, lesional and non-lesional oral mucosa, and feces (16S-S, 16S-L, 16S-NL, 16S-F), salivary and serum cytokines (CYT-S, CYT-Se), salivary and fecal metabolomics (MET-S, MET-F), as well as serum metabolites and lipoproteins (MET-Se, LIP-Se). **a**. Proportion of variance explained within each omics layer (i.e., view) by the full MOFA model, indicating the extent to which latent factors capture variability within each view. **b**. Variance explained (R^2) within each omics layer stratified by latent factor, showing how much variability within each molecular layer is captured by each latent factor. **c-e**. Top-weighted features associated with Factor 1 (**c**), Factor 2 (**d**) and Factor 3 (**e**). For each factor, the five features with the highest absolute weights (|weight|>0.1) were selected independently within each omics layer. Feature-factor edges are colored according to the sign of the weight, indicating positive or negative association with the corresponding factor. Feature node size is proportional to the absolute value of the weight, while label transparency further reflects feature magnitude. Omics layer node sizes are proportional to the variance explained (R^2) by the corresponding factor, providing a visual summary of factor-specific variance distribution across views. Phylum-level average relative abundance profiles in saliva (S), OLP-lesional mucosa (L), non-lesional mucosa (NL), and feces (F) specimens before (PRE) and after the 16-week intervention period (POST).

2.8.2. Factor 1

Factor 1 captured coordinated variance across serum lipoproteins, oral and gut microbiome profiles (mainly 16S-L and 16S-NL), and salivary cytokines (**Figure 7b**).

© 2026 by the author(s). Distributed under a Creative Commons CC BY license.

Preprints.org (www.preprints.org) | NOT PEER-REVIEWED | Posted: 22 May 2026 doi:10.20944/preprints202605.1565.v1

Higher Factor 1 scores were associated with negative weights for HDL-related components (Apo A1, Apo A1/HDL, HDL cholesterol, HDL phospholipids) and positive weights for VLDL triglycerides.

Microbial weights were distributed across oral and fecal genera with mixed directions across compartments, while salivary cytokines (including IL-33, IL-4, TNF-α, IL-21, and IL-25) consistently showed negative weights (**Figure 7c**).

Overall, Factor 1 delineates a coordinated axis linking systemic lipid remodeling with microbial variation across oral and fecal niches, accompanied by inverse shifts in salivary cytokines.

2.8.3. Factor 2

Factor 2 was primarily driven by metabolomics (MET-S and MET-F), with smaller contributions from microbiome views and limited involvement of salivary cytokines (**Figure 7b).**

Higher Factor 2 scores were characterized by positive weights for salivary metabolites such as indole-3-propionic acid, leucylglycine, and 4-aminobenzoic acid, and negative weights for α-tocopheryl acetate. Fecal metabolomics also contributed positively through amino acids including phenylalanine, β-alanine, and L-asparagine (**Figure 7d**).

Microbial contributions spanned oral and fecal genera (*e.g.*, *Actinomyces*, *Olsenella*, *Bulleidia*, *Blautia*, *Anaerostipes*), while salivary cytokine involvement was limited and positive (TGF-β2 and IL-23).

Collectively, Factor 2 represents a metabolite-dominant axis with partial microbial and limited cytokine contributions.

2.8.4. Factor 3

Factor 3 was mainly supported by salivary metabolomics (MET-S) and salivary cytokines (CYT-S), with smaller contributions from microbiome views and minimal input from fecal metabolomics (**Figure 7b**).

Higher Factor 3 scores were characterized by consistently positive weights for salivary cytokines, including IL-4, IL-33, IL-25, IL-6, and IL-31. In contrast, the top-weighted salivary metabolites (4′-hydroxyacetophenone, 4-cyanophenol, 2,3,4-trihydroxybutyric acid, N-(trimethylsilyl)hexanamide, cinnamic acid) displayed negative weights (**Figure 7e**).

Microbial weights were distributed across oral and fecal genera without a single dominant compartment.

Overall, Factor 3 delineates a localized salivary inflammatory axis characterized by coordinated cytokine increases and inverse shifts in specific salivary metabolites.

3. Discussion

OLP is a complex inflammatory immune-based disorder with an unclear etiology and an estimated risk of transformation to OSCC up to about 5%. Unfortunately, only limited therapeutic options are available, but emerging evidence suggests that its management may benefit from adjunctive vitamin D and/or targeted probiotic interventions. Indeed, vitamin D deficiency has been increasingly recognized as a potentially important and often overlooked factor in the pathogenesis of OLP. As reported in literature, its supplementation leads to preventive and therapeutic action by both suppressing pro-inflammatory cascades [35] and oral keratinocyte apoptosis [36]. Several longitudinal analyses have also explored the use of probiotics in OLP patients. For instance, Li et al. reported that *Streptococcus salivarius* K12 improves clinical outcomes, whereas Keller and Kragelund found that *Lactobacillus reuteri* DSM 17938 and ATCC PTA 5289 has no significant effect on the oral microbiota when administered alongside conventional OLP treatment [21,37]. Similarly, Marlina et al. evaluated the supplementation of a probiotic blend in a cohort of OLP patients, but no notable clinical or microbial improvements was observed [38]. The effects of probiotics in OLP remain inconsistent, likely due to differences in strains, dosage, treatment duration, and patient characteristics.

© 2026 by the author(s). Distributed under a Creative Commons CC BY license.

Preprints.org (www.preprints.org) | NOT PEER-REVIEWED | Posted: 22 May 2026 doi:10.20944/preprints202605.1565.v1

Recent studies have begun to explore the combined use of vitamin D and probiotics in both human and experimental OLP models, investigating whether their synergistic effects could enhance clinical outcomes and modulate the inflammatory response more effectively than either intervention alone. Nevertheless, the evidence remains limited and inconsistent, highlighting the need for well-designed controlled trials to determine whether co-administration offers advantages over single interventions [39,40].

To address these gaps, we previously conducted two in vitro studies. First, we screened various *Lactobacillus* and *Bifidobacterium* strains against human oral pathobionts (*Aggregatibacter actinomycetemcomitans*, *Streptococcus mitis*, and *Streptococcus mutans*) [41]. Then, we assessed the effects of the selected *L. reuteri* LRE11, *L. rhamnosus* LR04, and *L. casei* LC04 strains, together with their co-culture cell-free supernatants (CFSs) and vitamin D, on the viability and IL-6 production of oral epithelial FaDu cells infected with *A. actinomycetemcomitans*, *Fusobacterium nucleatum*, and *Porphyromonas gingivalis* [28]. Based on the evidence obtained from these in vitro studies, the aim of the present study was to in vivo evaluate the translational potential of a probiotic blend, comprising LRE11, LR04, and LC04, combined with vitamin D on a cohort of 25 OLP patients through a comprehensive clinical assessment integrated with multi-omics analyses, thus providing the first evidence of its clinical efficacy in OLP. Notably, this approach greatly differs from previous studies since it incorporates context-specific preclinical validation to guide strain selection, thereby providing a stronger mechanistic rationale for the observed effects.

3.1. Overview and Clinical Efficacy

The primary clinical outcome of this monocentric pilot study was highly encouraging, with a significant reduction in lesion number (p<0.001), largest lesion size (p=0.004), and bleeding burden (p=0.014). Moreover, the composite Clinical Activity Index confirmed that overall remission was the predominant clinical outcome (76% of the patients, p<0.001), reflecting broad disease stabilization and recovery. The baseline profile of the cohort, characterized by high prevalence of erosive lesions (44%) and systemic medication inducing xerostomia (72%) [42], further highlights the clinical relevance of these findings.

This clinical improvement is associated with a significant increase in serum vitamin D levels over the 16-week period, particularly in patients who initiated supplementation during the study (p<0.01), thus strongly supporting the treatment efficacy. Several studies have linked vitamin D deficiency to OLP pathogenesis, as well as to disease severity and progression to oral cancer [43–45]. Specifically, lower serum vitamin D levels have been reported in patients with the erosive form of OLP [43], as well as in symptomatic individuals [46]. Given these premises, the restoration of adequate vitamin D levels likely contributed to the observed therapeutic effects, potentially synergizing with the immunomodulatory properties of the selected probiotic blend.

3.2. Immune Modulation

To determine whether the observed clinical benefits were mirrored at the molecular level, we next analyzed inflammatory salivary and serum cytokine markers in our OLP cohort. Although PRE vs POST changes did not reach formal statistical significance after correction for multiple comparisons, the pattern and size of the shifts remain clinically meaningful in a small exploratory cohort. The pattern of variation suggests that intervention primarily modulates the local inflammatory oral environment rather than systemic immune responses. Notably, IL-21 and IL-33 are key mediators of the Th17 and alarmin pathways, respectively. The former is involved in sustaining chronic mucosal inflammation [47], whereas the latter is associated with damaged epithelial cells and amplifies the inflammatory cascade [48]. The reduction of these cytokines in saliva at POST may reflect an improvement of the oral epithelium and an attenuation in T-lymphocyte activation and local inflammatory processes, therefore mirroring and/or potentially contributing to the observed clinical improvements. Furthermore, the salivary cytokine patterns observed here are mechanistically consistent with the anti-inflammatory properties documented in vitro [28],

© 2026 by the author(s). Distributed under a Creative Commons CC BY license.

Preprints.org (www.preprints.org) | NOT PEER-REVIEWED | Posted: 22 May 2026 doi:10.20944/preprints202605.1565.v1

suggesting translational continuity from bench to clinic and supporting the hypothesis that strain-specific immunomodulation of the oral mucosa is a prerequisite for clinical efficacy in OLP.

3.3. Serum Lipid Profile

OLP has been shown to be positively associated with dyslipidemia [49,50]. In parallel, accumulating clinical evidence indicates that probiotic supplementation may contribute to the modulation of circulating lipid profiles, with reported reductions of TC, TG, LDL-C levels and improved HDL-C levels [51].

In our cohort, we did not identify statistically significant changes in lipoprotein fractions; however, the descriptive patterns point to a subtle remodelling of lipoprotein metabolism following vitamin D and probiotic blend treatment, characterized by increased phospholipids levels in VLDL1 and elevated triglycerides in both IDL and VLDL1, paired with lower triglycerides in LDL and LDL1 fractions. However, the observed increases in several triglyceride-rich lipoprotein particles contrast with the existing literature and may be specifically associated with OLP patients. The observed increases in triglyceride-rich lipoprotein particles contrast with previous reports of lipid-lowering effects of vitamin D and probiotics. This discrepancy may reflect unique metabolic alterations in OLP patients, potentially driven by chronic low-grade inflammation or disease-specific lipid handling [52,53]. Given the small size of our cohort, these results should be interpreted cautiously, but they highlight a possible link between OLP-associated inflammation and lipoprotein remodeling. Taken together, these observations warrant further investigation in larger cohorts to clarify their metabolic and clinical relevance.

3.4. Metabolic Reprogramming of the Gut-Oral Axis

Untargeted metabolomic profiling of saliva and feces indicates that supplementation was associated with axis-level metabolic reprogramming. Saliva showed a net depletion of significant metabolites (69 decreased vs 16 increased), whereas feces showed relative enrichment (18 increased vs 16 decreased), consistent with redistribution of substrates and microbial end-products between two connected mucosal ecosystems linked by swallowing and systemic exchange along the oral–gut axis [54]. In the oral compartment, the dominant signal was reduced availability of free amino acids and carbohydrates/polyols, including a marked drop in threonine and lower branched-chain amino acids (leucine, valine) alongside decreases in mannose, arabinose and 1,5-anhydroglucitol. Threonine is a major constituent of mucin glycoproteins and can become limiting when barrier turnover is increased; thus, lower salivary threonine may reflect intervention-associated shifts in epithelial repair demand and/or microbial amino-acid routing within the oral niche [55]. Concomitant decreases in indole/tryptophan-related metabolites (indole-3-acetic acid and anthranilic acid) point to altered microbial tryptophan catabolism; indole metabolites are well-established AhR ligands that support epithelial barrier programs and modulate mucosal inflammation [56]. Despite depletion of many substrates, saliva increased in malonic acid, diglycerol and hippurate, together with enrichment of glycolysis/pyruvate and glycerolipid pathways, suggesting rerouting of central carbon and lipid turnover rather than simple “metabolic suppression”.

In feces, pathway impact centered on glycine/serine/threonine and alanine–aspartate–glutamate nodes, indicating coordinated remodeling of luminal nitrogen networks. Decreased β-hydroxybutyrate is notable because this ketone can inhibit NLRP3 inflammasome activation [57]; reduced fecal abundance could reflect increased host uptake or altered fermentation output. The reduction in pimelic acid, a precursor in bacterial biotin (vitamin B7) biosynthesis, suggests altered microbial biosynthetic fluxes connected to fatty-acid-derived metabolism [58]. Conversely, increases in niacinamide implicate nicotinamide/NAD+-related metabolism, a host–microbe interface increasingly linked to inflammatory and metabolic states [59,60].

Taken together, the saliva-feces divergence supports the concept that supplementation shifts host-microbe co-metabolism across the gut-oral axis, potentially changing the metabolite “inputs” arriving at the oral mucosa via circulation and entero-oral transport [54].

© 2026 by the author(s). Distributed under a Creative Commons CC BY license.

Preprints.org (www.preprints.org) | NOT PEER-REVIEWED | Posted: 22 May 2026 doi:10.20944/preprints202605.1565.v1

3.5. Site-Specific Microbiota Remodelling Across Oral and Gut Compartments

An important feature of this study is the comparison of metagenomics data across the different specimens. Indeed, the analysis shows a marked specimen-specific composition of the microbiota, with oral and stool communities displaying the greatest differences in biodiversity, structure, and response to the intervention.

As expected, at baseline stool samples are richer and more uniform than oral samples (approximately 160 versus 120 microbial features, respectively), reflecting the higher ecological complexity of the gut niche. Overall, the microbial composition shows typical physiological patterns, with Bacillota and Actinomycetota phyla dominating the oral sites, and Bacteroidota constituting a major component of the gut microbiota.

α-diversity analysis revealed no statistically significant differences between PRE and POST across all specimens. However, the biodiversity indices show an upward trend of microbial richness upon intervention. This trend is more pronounced in saliva, followed by lesional mucosa and stool samples; in contrast, non-lesional mucosa exhibits minimal temporal variation.

In terms of β-diversity, while the body site remains the dominant factor shaping the global microbiome profile (explaining ~51% of variance), the intervention successfully induces a statistically significant shift in microbial composition across all specimens.

To dissect these global shifts, differential abundance analysis was performed, revealing significant microbial signatures in all specimens.

In particular, the salivary microbiota exhibits the greatest shift upon probiotic supplementation, consistently with α- and β-diversity data. We observed a significant reduction in *Lancefieldella* (formerly *Atopobium*, Actinomycetota) and *Bulleidia* (Bacillota), commonly linked to oral dysbiosis and related disorders (periodontitis and caries, respectively) [61]. Indeed, OLP and periodontitis often coexist, establishing a vicious mechanism that could lead to precancerous lesions in OLP patients [62]. The reduction of the above-mentioned genera upon intervention could support two complementary interpretations. On the one hand, it may reflect the active competitive antagonism between the probiotic blend and periodontal pathogens through modulation of immune inflammatory pathways and inhibition of their growth [63]. Conversely, their decrease might also indicate a progressive improvement in oral eubiosis. This is lined with the concomitant significant increase in *Neisseria* (Pseudomonadota), a core oral commensal [64], *Cloacibacterium* (Bacteroidota), a member of the healthy laryngeal microbiome [65] and *Pseudoleptotrichia* (Fusobacteriota) genera. However, these findings remain inconclusive, since elevated levels of *Neisseria* have been also found in saliva from erosive OLP patients [66], whereas *Pseudoleptotrichia goodfellowii*, the only member of the *Pseudoleptotrichia* genus, contributes to dental biofilm [67]. The significant enrichment in *Arcobacter* (Campylobacterota), which includes both commensal and pathogenic species, detected in saliva and plaques from OSCC patients [68,69], warrants careful interpretation, too. These findings align with expectations, as many oral bacteria exhibit context-dependent function. They may behave as commensals within an eubiotic microbial network; yet, favored by exposome-driven selection [70], they may contribute to dysbiosis and inflammation. In such altered ecosystems, these microbes often express virulence not as overt pathogenicity, but as adaptive survival strategies within the microbial network [71].

The mucosal microbiota is of great interest, as dysbiosis seems to be more marked within this site than in the saliva of OLP subjects and more closely associated with disease features [2,72]. In lesional mucosa, we observed upon treatment a significant enrichment in genera belonging to Bacillota (*Lacticaseibacillus*), Bacteroidota (*Chryseobacterium*), Campylobacterota (*Arcobacter*), and Pseudomonadota (*Acetobacter*) phyla. The increase in *Arcobacter* and *Acetobacter* genera mimic the trend previously observed in saliva.

Interestingly, the intervention seems to affect also non-lesional specimens, as we could observe a significant enrichment in exclusive taxa from Actinomycetota, Bacteroidota, and Fusobacteriota (*e.g.*, *Slackia*, unclassified Weeksellaceae, and *Leptotrichia*). The latter was previously found to be more abundant in OLP buccal microbiota compared to healthy controls; however, the Authors did not specify whether mucosa samples were lesional or not [73]. The absence of significant bacterial

© 2026 by the author(s). Distributed under a Creative Commons CC BY license.

Preprints.org (www.preprints.org) | NOT PEER-REVIEWED | Posted: 22 May 2026 doi:10.20944/preprints202605.1565.v1

decreases in mucosal specimens suggests that the probiotic intervention does not competitively displace existing colonizers, but rather improves complexity of the mucosal microbiota, without disrupting established commensal networks.

Remarkably, the significant enrichment in *Lacticaseibacillus* genus in saliva and lesional specimens is consistent with the composition of the probiotic supplementation, suggesting successful colonization or transient enrichment in the oral cavity. As discussed, their presence could sustain mucosal barrier function and immune modulation, thus creating favourable conditions for microbial restoration [74,75].

Conversely, the gut microbiota shows only mild changes, consistent with the oral route of the probiotic administration, involving a mouthwash and, thereby, exposing the oral mucosa directly to the probiotic blend. Nevertheless, the increase of *Lacticaseibacillus* and *Limosilactobacillus* genera (Bacillota) might indicate the capability of the related probiotic strains to successfully survive gastrointestinal passage and transiently enrich the intestinal ecosystem. Changes in the gut microbial community were substantially milder than in the oral cavity, suggesting that the primary microbial impact occurred at the delivery site. This modest gut response may also reflect the resilience of the established gut microbiome to temporary perturbations, especially in the absence of strong exogenous factors, *e.g.*, anthropogenic antibiotics [76].

These findings suggest that the intervention primarily promotes microbial compositional remodeling rather than diversity expansion, with both size and direction of the microbial shifts strongly influenced by the anatomical site and local ecological context. While the 16-week intervention period is considered sufficient to capture changes in the microbial community structure, detectable alterations in β-diversity were more pronounced than changes in α-diversity. High inter-individual variability and the complexity of host-microbiome interaction may limit statistical significance of diversity metrics in probiotic trials [77]. Taken together, these results indicate that the intervention exerts multifaceted effects at the molecular, immunological, and metabolic levels, which may support the clinical benefits observed in our OLP cohort, highlighting the potential of targeted probiotic and vitamin D supplementation to modulate local inflammation and host metabolic pathways.

3.6. Serum Lipid Profile

OLP is a highly complex disease requiring a system-level perspective which cannot be fully captured through univariate approaches. Therefore, the application of MOFA allowed us to provide a comprehensive view of the coordinated molecular changes, identifying latent factors summarizing shared sources of variation across the immune, metabolomics, and metagenomics layers.

In practical terms, the latent factors captured the largest proportions of measurable change in oral and intestinal readouts (particularly salivary metabolomics, lesional microbiota, fecal metabolomics, and salivary cytokines), whereas blood-based cytokines and metabolites showed much smaller shifts. This pattern further validates the involvement of a gut-oral-immune axis and reveals a coordinated multi-compartment process that extends beyond localized oral inflammation.

Indeed, Factor 1 links salivary cytokines, serum lipid fractions, and microbial shifts across oral and gut niches. This reinforces the mucosa-driven gut-oral-immune axis, suggesting that oral T-cell/alarmin dampening synchronizes with lipid remodelling, potentially modulated by restored vitamin D levels and gut-liver crosstalk [52]. Additionally, higher Factor 1 scores characterized patients with commensal/fermentative bacteria enrichment across oral and gut sites alongside reduced oral pathobionts (*e.g.*, *Bulleidia*, *Selenomonas*).

Factor 2 predominantly captures metabolic adaptation. Several salivary metabolites show positive weights, such as indole-3-propionic acid (IPA). IPA is a gut microbiota-derived catabolite of tryptophan, whose anti-inflammatory and immunomodulatory properties are well recognised [78]. Its co-occurrence with specific amino acids (phenylalanine, beta-alanine) and gut-associated genera (*e.g.*, *Blautia*, *Anaerostipes*) suggests a metabolic fingerprint of gut-health-promoting bacteria. Furthermore, the involvement of oral taxa (*e.g.*, *Actinomyces*, *Olsenella*) in this factor highlights the

© 2026 by the author(s). Distributed under a Creative Commons CC BY license.

Preprints.org (www.preprints.org) | NOT PEER-REVIEWED | Posted: 22 May 2026 doi:10.20944/preprints202605.1565.v1

close connection between the oral and intestinal communities, as they share both metabolic byproducts and microbial signals.

Factor 3 focuses more on the oral cavity, stressing the pivotal role of MET-S and CYT-S readouts. The inverse relationship between these inflammatory markers (Th2 and alarmin pathways) and salivary metabolites is noteworthy. Cinnamic acid and 4'-hydroxyacetophenone are often associated with antioxidant properties and gut microbial degradation of polyphenols [79,80]. The reduction of these metabolites, coupled with raised inflammatory markers, points to either a disruption in beneficial microbial metabolism or a more oxidative environment that depletes these compounds. Consequently, this dynamic reveals a potential 'molecular switch' within the oral cavity, wherein the loss of metabolic stabilizers triggers the onset of mucosal inflammation.

A key insight from MOFA is the distinction between 'abundance' and 'influence.' Indeed, the *Lacticaseibacillus* genus showed a significant increase in abundance at POST according to univariate analysis. However, its lack of contribution to the MOFA factor highlighted that the observed systemic therapeutic effects should not be attributed solely to probiotic abundance per se. Rather, the clinical response appears to reflect a broader multi-layer reorganization involving microbial, metabolic, and immune components. Within this scenario, we could hypothesize that the probiotic blend may act as a keystone modulator, both directly and indirectly, triggering the complex cascade of metabolic reprogramming that extends far beyond their colonization of the gut or oral cavity.

Combining differential abundance with MOFA provided a comprehensive view of microbial dynamics, capturing both significant taxonomic shifts and the latent biological axes that organize these changes across multiple molecular layers. However, it is important to acknowledge certain methodological constraints. As MOFA is based on linear relationships, it may not fully capture nonlinear interactions and may remain sensitive to residual technical artifacts or preprocessing choices. Moreover, the latent factors should be interpreted as compact summaries of multi-omics covariation rather than as evidence of causality. Nevertheless, these factors offer a useful framework for generating biologically informed hypotheses on microbiota-metabolism-immunity links. Overall, our results indicate that the main latent structure was predominantly shaped by coordinated variation across microbiome and metabolomics layers, with more selective contributions from immune and lipid-related features.

3.7. Limitations

Despite the promising findings of our study, some limitations must be acknowledged.

First, the relatively small sample size and the single-centre design may limit the generalizability of the results and increase the risk of selection bias. Although the PRE–POST design enables a detailed intra-subject comparison, thus partially mitigating inter-individual variability, it doesn't provide the same level of causal inference as a randomized controlled trial.

Another major limitation is the absence of a placebo control group, which precludes a definitive attribution of the observed clinical improvements solely to the intervention. Furthermore, treatment protocols were not uniform across the cohort. Specifically, only a subset of patients received Vitamin D supplementation, making it difficult to isolate its independent clinical effects and separate the specific contribution of each component of the combined therapy.

Moreover, the study population presented with a high prevalence of comorbidities and was subject to various concurrent pharmacological treatments that could independently influence the disease course, thereby acting as significant confounding factors.

To partially mitigate these limitations, we employed mixed-effects models to adjust for baseline patient characteristics, but residual confounding cannot be entirely ruled out. Consequently, our findings must be interpreted with caution. The current study serves primarily an exploratory purpose, providing hypothesis-generating data that require validation through future robust, randomized controlled clinical trials.

4. Materials and Methods

© 2026 by the author(s). Distributed under a Creative Commons CC BY license.

Preprints.org (www.preprints.org) | NOT PEER-REVIEWED | Posted: 22 May 2026 doi:10.20944/preprints202605.1565.v1

4.1. Ethical Issues

The study protocol, conducted as a pilot clinical investigation, was approved by the Ethics Committee (Comitato Etico Interaziendale, CEI) of the Azienda Ospedaliero-Universitaria (AOU) Maggiore della Carità (Novara, Italy) serving as an Institutional Review Board (IRB) (Protocol Number 801/CE, Approval Study Number CE 143/21), in accordance with the Declaration of Helsinki and its Edinburgh amendments [81].

This study was conducted as a pilot clinical investigation and was not registered on ClinicalTrials.gov or any other public registry.

4.2. Study Population

Twenty-five adult OLP patients (clinical and histopathological diagnosis) were enrolled at the Odontostomatology Unit of AOU Maggiore della Carità, during the May-September period, after obtaining their written informed consent and securing agreement from their family doctor.

The inclusion criteria were as follows: patient's age ≥ 18 years, neither current corticosteroid and/or antibiotic treatments, nor probiotic supplementation for at least one month prior to enrollment and throughout the study.

4.3. Vitamin D and Probiotic Supplementation

Baseline vitamin D levels were assessed upon enrollment. Only patients with vitamin D deficiency (10-20 ng/mL) at baseline were supplemented with 2,000 IU/day of Vita D3 (2 tablets/day, Erba Vita Group S.p.A., San Marino, Italy) for 16 weeks.

Based on previous *in vitro* analyses [41], patients received a lyophilized probiotic mixture, containing *Limosilactobacillus reuteri* LRE11 (DSM 33827), *Lacticasebacillus rhamnosus* LR04 (DSM 16605), and *Lacticasebacillus casei* LC04 (DSM 33400), at 1 x 10^9 Active Fluorescent Units (AFU) & Colony Forming Units (CFU)/g/day with maltodextrin (Probiotical Research S.r.l., Novara, Italy) for 16 weeks. The probiotic mixture was dissolved in lukewarm water, used as an oral rinse for 30 seconds (s), and then swallowed. A telephonic follow-up was conducted every 4 weeks to ensure proper adherence to the supplementation regimen.

4.4. Data Collection

For each enrolled patient, a comprehensive set of variables was collected before (PRE) and after the 16-week intervention (POST). These included: (i) demographic information (*e.g.*, age, sex, body mass index (BMI)); (ii) OLP-related clinical features and histopathology (*e.g.*, lesion form, lesion number, lesion size, affected sites); (iii) medical history, comorbidities, and ongoing medications.

Biological samples were collected at PRE and POST. At each time point, multiple specimen types were collected for each patient to enable comprehensive multi-omics analyses, including serum (SE), saliva (S, unstimulated and oral swab), OLP-lesional mucosa (L, oral swabs and photographs), non-lesional mucosa (NL, oral swabs), and feces (F).

For oral cavity related biological samples, patients were instructed to avoid eating (including chewing gum), drinking, smoking, or performing oral hygiene for at least 2 hours before each visit to prevent inaccurate results.

4.4.1. Serum Samples

Two serum 2.5 mL samples were collected from each patient and time point. One sample was used for vitamin D quantification in the same hospital. The other sample was centrifuged at 3,000 × g for 10 minutes (min) at room temperature (RT), aliquoted, and stored at -80 °C for cytokine and metabolomics analysis.

4.4.2. Saliva Samples

© 2026 by the author(s). Distributed under a Creative Commons CC BY license.

Preprints.org (www.preprints.org) | NOT PEER-REVIEWED | Posted: 22 May 2026 doi:10.20944/preprints202605.1565.v1

For saliva collection, two mL unstimulated saliva (*i.e.*, saliva naturally secreted by the salivary glands in the absence of any stimulation) samples were collected in the morning without oral cleaning and under fast conditions, placed into polypropylene sterile tubes (Biosigma, Cona, Italia), kept at 4 °C, and processed within 2 hours. Briefly, the saliva samples were centrifuged at 2,500 × g for 15 min at 4 °C, then aliquoted and stored at -80 °C for cytokine and proteomics analysis.

4.4.3. Oral Swabs

e-NAT® swabs (Copan Italia, Brescia, Italy) containing 1 mL of nucleic acid stabilizing solution were used to collect patient's oral swabs from S, L, and NL. Samples were kept at RT and processed within 2 hours (h) by centrifugation at 1,000 × g for 2 min at RT, then stored at -80 °C until microbiome analysis.

4.4.4. Stool Samples

Fecal samples were collected in appropriate containers, kept at 4 °C, and processed within 2 h. Each sample was aliquoted into 2 mL Eppendorf tubes and stored at -80 °C until gut microbiota and proteomics analysis.

4.5. OLP Severity and Clinical Activity

4.5.1. Baseline Severity Classification

At baseline, patients were grouped into three severity categories according to lesion type reflecting differences in inflammation and symptom burden: Severe (erosive/ulcerative lesions), Mild-Severe (papular, plaque-like, or atrophic lesions without erosive lesions), and Mild (reticular lesions only).

4.5.2. Clinical Activity Assessment

For each patient, lesions were evaluated in terms of number, size, and bleeding status. These parameters were used to assess clinical activity changes during the intervention period. A composite Clinical Activity Index was constructed by mapping each marker to a numerical score (−1 for remission, 0 for stability, +1 for recurrence) and summing scores across markers for each patient. Patients were then classified as experiencing overall remission (index < 0), stability (index = 0), or recurrence (index > 0).

4.6. Salivary and Serum Cytokines

4.6.1. Cytokine Profiling

To assess the patient's inflammatory status, a multiplex immunoassay was performed. Cytokine levels, including IL-1β, IL-4, IL-6, IL-10, IL-17A, IL-17F, IL-21, IL-22, IL-23, IL-25, IL-31, IL-33, IFN-γ, soluble CD40 ligand (sCD40L), tumor necrosis factor alpha (TNFα), and TGF-β1, TGF-β2, TGF-β3, were quantified in unstimulated saliva and serum samples. Analyses were performed by the Protein Technologies Core Facility at UPO-CAAD using the Bio-Plex Pro™ Human Th17 Cytokine Panel 15-Plex and Bio-Plex™ TGF-β Assays (Bio-Rad, Segrate, Milan, Italy) and the Bio-Plex 200 System (Bio-Rad, Segrate, Milan, Italy), according to the manufacturer's instructions.

4.7. Serum Metabolomics Analysis

4.7.1. Sample Preparation and Nuclear Magnetic Resonance (NMR) Analysis

Serum samples were prepared and analyzed according to standard protocols [82,83]. ^{1}H NMR spectra were obtained using a Bruker 600 MHz spectrometer (Bruker BioSpin, Ettlingen, Germany), operating at a proton Larmor frequency of 600.13 MHz. The spectrometer was equipped with a 5 mm PATXI ^{1}H-^{13}C-^{15}N probe, a z-axis gradient coil, an automatic tuning and matching (ATM) unit, and

© 2026 by the author(s). Distributed under a Creative Commons CC BY license.

Preprints.org (www.preprints.org) | NOT PEER-REVIEWED | Posted: 22 May 2026 doi:10.20944/preprints202605.1565.v1

an automatic refrigerated sample changer (SampleJet, Bruker BioSpin) maintained at 6 °C. Temperature stabilization during measurement was controlled by a BTO 2000 thermocouple, ensuring an accuracy of approximately 0.1 K.

Prior to data acquisition, samples were equilibrated in the NMR probe at 310 K for at least 300 s. Spectrometer calibration followed daily standard operating procedures to ensure spectral quality and reproducibility [84]. For each sample, a standard nuclear Overhauser effect spectroscopy (NOESY) sequence was applied with the following parameters: 32 scans, 98,304 data points, spectral width of 18,028 Hz, acquisition time of 2.7 s, relaxation delay of 4 s, and a mixing time of 0.01 s [85]. This setup allowed for the detection of both high molecular weight (MW) molecules (*e.g.*, lipoproteins, proteins, lipids) and low MW metabolites. Prior to Fourier transformation, free induction decays were processed with an exponential function to achieve a line-broadening factor of 0.3 Hz. Transformed spectra were automatically corrected for phase and baseline distortions, then calibrated to the glucose anomeric doublet at δ 5.24 ppm using TopSpin 3.6.2 software (Bruker BioSpin).

4.7.2. Quantification of Serum Metabolites and Lipoproteins

A total of 24 metabolites identified were quantified in all spectra using the Bruker IVDr Quantification platform for Plasma/Serum (B.I.Quant-PS™, Bruker BioSpin) [86]. Additionally, 112 lipoprotein-related parameters were analyzed with the Bruker IVDr Lipoprotein Subclass Analysis platform™ (version 1.0.0, Bruker BioSpin). This analysis covered lipoprotein components within the primary VLDL, IDL, LDL, and HDL classes, including six subclasses of VLDL (VLDL-1 to VLDL-6, ordered by increasing density and decreasing size), six LDL subclasses (LDL-1 to LDL-6), and four HDL subclasses (HDL-1 to HDL-4). For each main lipoprotein class and subclass, concentrations of triglycerides, cholesterol, free cholesterol, phospholipids, Apo-A1, Apo-A2, and Apo-B100 were calculated.

4.8. Saliva and Fecal Metabolomics Analysis

4.8.1. Sample Preparation and MS Analysis

Analyses were performed by the Metabolism Core Facility at UPO-CAAD. To 500 µL of saliva, 700 µL of ice-cold acetonitrile were added. Samples were then centrifuged at RT at 15000xg for 5 min. Supernatants were collected and transferred to a new tube, then dried in a speed vacuum and stored at -20°C until derivatization.

Molecules were extracted from stool samples using a 1 mL mixture of acetonitrile (ACN), isopropanol (IPA), and water 3:3:2, with 5 µL of tridecanoic acid (0.5 mg/mL), 5 µL of palmitic acid d31 (0.5 mg/mL), 5 µL of stearic acid d35 (0.5 mg/mL), 3.5 µL of glycine d4 (10.07 mg/mL) as internal standards. After being vortexed, the sample was centrifuged for 15 min at 20 °C at 14500x g. Next, 1 mL of the supernatant was dried in a speed vacuum at 40°C and stored at -20 °C until derivatization.

Derivatization was performed on saliva and fecal samples with a first step of methoximation (20 µL of methoxamine at 80 °C for 20 min) and a second step of silylation (30 µL of N,O-Bis(trimethylsilyl)trifluoroacetamide at 80 °C for 20 min).

For metabolomics profiling, a LECO Pegasus BT 4D GC×GC-TOFMS system equipped with a dual-stage quad jet thermal modulator (LECO Corp., St. Joseph, MI, USA) was used. The first-dimension separation was performed on a 30 m Rxi-5Sil MS capillary column (Restek Corp., Bellefonte, PA, USA; 0.25 mm i.d., 0.25 µm film), coupled to a 2 m Rxi-17Sil MS secondary column (Restek Corp.) with identical internal diameter and film thickness. High-purity helium (99.9999%) was employed as the carrier gas at a constant flow of 1.4 mL/min. As described by Barberis et al. [87], 1 µL of each derivatized sample was injected in splitless mode at 250 °C. The primary oven temperature program was: 70 °C (2 min), then ramped at 6 °C/min to 160 °C, 10 °C/min to 240 °C, and 20 °C/min to 300 °C, with a final hold of 6 min. The secondary oven was maintained 20 °C above the primary oven, using the same temperature ramp. Electron impact ionization (70 eV) was applied, with the ion source at 250 °C. Spectra were acquired over m/z 25–550 at 200 spectra/s, with a

© 2026 by the author(s). Distributed under a Creative Commons CC BY license.

Preprints.org (www.preprints.org) | NOT PEER-REVIEWED | Posted: 22 May 2026 doi:10.20944/preprints202605.1565.v1

modulation period of 4 s, an extraction frequency of 32 kHz, a modulator temperature offset of +15 °C relative to the secondary oven, and a transfer line temperature of 280 °C. Chromatograms were collected in TIC mode.

4.8.2. Quantification of Salivary and Fecal Metabolites

ChromaTOF version 5.54 was used for raw data processing. Mass spectral assignment was performed by matching with NIST MS Search 2.3 libraries and the FiehnLib. In addition, an in-house library of standards was used to identify small molecules.

4.9. 16S Metabarcoding

4.9.1. DNA Isolation

To avoid contamination, microbial DNA extraction was performed under sterile conditions using a laminar flow cabinet, sterile reagents and materials in agreement with good scientific practices.

4.9.1.1. Oral Microbiota

Swabs from unstimulated saliva, OLP lesions, and non-lesional mucosa were thawed for bacterial DNA extraction using the QIAamp® DNA Microbiome Kit (Qiagen, Hilden, Germany), following the manufacturer's instructions. DNA concentration was fluorimetrically measured using the Qubit™ 1X dsDNA HS Assay Kit (Invitrogen Co., Thermo Fisher Scientific Inc., Walthman, MA, USA) on a Qubit™ 4 fluorometer (Invitrogen Co.).

4.9.1.2. Gut Microbiota

Stool samples were thawed at RT and subjected to bacterial DNA isolation using the QIAmp® PowerFecal® Pro DNA kit (Qiagen) according to the manufacturer's instructions. Yield and quality of bacterial DNA were assessed on a NanoDrop™ One/Onec spectrophotometer (Thermo Fisher Scientifics Inc.).

4.9.2. Sequencing

DNA samples (from S, L, NL, and F) were analyzed by 16S rRNA gene metabarcoding to compare microbial composition and relative abundances across the different biological matrices before (PRE) and after (POST) the intervention. Library preparation and sequencing were performed by the Integrative Genomics Core Facility at UPO-CAAD using CE-IVD kits (Arrow Diagnostics S.r.l., Genoa, Italy). The AD4SEQ Microbiota Solution A Kit was used for bacterial DNA isolated from S, L, and NL samples (V1–V3 hypervariable regions), whereas the AD4SEQ Microbiota Solution B Kit was applied to F samples (V3–V4–V6 hypervariable regions).

PCR amplification of the selected hypervariable regions was performed with degenerate primers following the manufacturer's instructions. Amplicons were purified using Agencourt AMPure XP magnetic beads (Beckman Coulter Inc., Brea, CA, USA) and indexed in a subsequent step. DNA concentration of the libraries was quantified fluorimetrically using the Qubit™ 1X dsDNA HS Assay Kit (Invitrogen Co., Thermo Fisher Scientific Inc.) and pooled in equimolar amounts. Sequencing was carried out on a MiSeq Illumina® platform with a MiSeq Reagent v2 cartridge (2 × 250 bp, paired-end) (all from Illumina, San Diego, CA, USA).

Control samples, including isolation and amplification controls, were processed in parallel with the biological samples.

4.9.3. Bioinformatics Analysis

Raw sequencing data were analyzed using MicrobAT Suite v1.2.1 (SmartSeq S.r.l., Novara, Italy), a standalone software for primary analysis and quality controls. Sequences shorter than 200 nucleotides or with low quality (average Phred score < 25) were discarded [88].

© 2026 by the author(s). Distributed under a Creative Commons CC BY license.

Preprints.org (www.preprints.org) | NOT PEER-REVIEWED | Posted: 22 May 2026 doi:10.20944/preprints202605.1565.v1

High-quality sequences were aligned against the Ribosomal Database Project (RDP, RDP_trainingsetNo19_2023-08-23) to assign taxonomy, applying a query coverage ≥ 80% and a similarity threshold ≥ 97% [89]. MicrobAT generated three output files (OTU, taxonomy and metadata) as input for downstream statistical analyses.

4.10. Statistical Analyses

All statistical analyses were performed in R (v4.5.1).

Lesion-related outcomes (lesion number, largest lesion size in cm, and number of bleeding lesions) were evaluated in a paired POST-PRE design. Differences were assessed using two-sided Wilcoxon signed-rank tests. For descriptive reporting and visualization, each endpoint was additionally categorized per patient as remission, stability, or recurrence based on the sign of Δ=POST-PRE (remission if Δ<0, stability if Δ=0, and recurrence if Δ>0). A composite Clinical Activity Index was constructed by mapping each marker to a numerical score (−1 for remission, 0 for stability, +1 for recurrence) and summing scores across markers for each patient; patients were classified as overall remission (index < 0), stability (index = 0), or recurrence (index > 0). The directional imbalance of the composite classification toward remission was evaluated using an exact binomial (sign) test comparing the number of patients in remission versus recurrence, excluding stable cases.

For cytokines (saliva and serum) and salivary and fecal metabolites, quantitative concentrations were analyzed on a log scale using log(x + offset), where the offset was defined as half of the minimum non-zero value within each analyte/feature. Serum metabolites and lipoproteins were analyzed on their original scale, as their distributions were substantially more stable compared to the other omics layers. Features detected in fewer than five samples were excluded prior to analysis.

Longitudinal changes were primarily assessed using linear mixed-effects models using lme4 (v1.1-38) [90] and, with time as the main fixed effect, adjustment for age, sex, BMI, baseline vitamin D level, baseline clinical severity, and a subject-specific random intercept to account for within-patient pairing. Model-based POST-PRE contrasts were computed with 95% confidence intervals and reported as back-transformed estimated marginal means on the original scale when appropriate (*e.g.*, pg/mL for cytokines). For multiple testing control within each outcome family (*e.g.*, cytokine panel, serum metabolite/lipoprotein set, salivary/fecal metabolite set, genus-level differential abundance per specimen), p-values were adjusted using the Benjamini-Hochberg false discovery rate (FDR) procedure, with an FDR threshold of 0.05 for declaring statistical significance.

Pathway analysis for salivary and fecal metabolomics data was performed using Metaboanalyst software v.6.0 (https://www.metaboanalyst.ca).

Microbiome analyses were conducted from MicrobAT outputs on S, L, NL, and F samples. Microbial abundances and taxonomy tables were imported into R, stored as TreeSummarizedExperiment objects, and analyzed using the mia package (v1.18) [91]. For each object separately, features classified as Eukaryota and those lacking a phylum-level taxonomic assignment were removed. To reduce sparsity and improve comparability across samples, taxa were agglomerated at the genus level. A prevalence filter was then applied to remove features present in less than 10% of samples to mitigate the impact of rare, sample-specific features that are more likely to reflect sampling stochasticity or technical artefacts than reproducible biological patterns. Relative abundances were computed and transformed using centered log-ratio (CLR) with a pseudocount equal to half of the minimum non-zero relative abundance within each dataset.

Within-sample diversity (genus richness, Shannon index, and dominance of the most abundant genus) was tested using linear mixed-effects models including specimen type, time, and their interaction as fixed effects, a random intercept for subject, and covariate adjustment as above. Post-hoc contrasts were restricted to (i) PRE-POST comparisons within each specimen type and (ii) between-specimen comparisons within each time point, and p-values for these contrasts were adjusted using the Šidák procedure.

Between-sample diversity was assessed using Aitchison distances on CLR-transformed data and visualized by principal coordinate analysis (PCoA); community-level effects of specimen type and

© 2026 by the author(s). Distributed under a Creative Commons CC BY license.

Preprints.org (www.preprints.org) | NOT PEER-REVIEWED | Posted: 22 May 2026 doi:10.20944/preprints202605.1565.v1

time were evaluated by PERMANOVA (adonis2 function of vegan package v2.7-2 [92], and homogeneity of dispersion was assessed to support the validity of PERMANOVA inferences.

Differential abundance testing was performed separately for each specimen type on genus-level CLR values using glmmTMB package (v1.1.13) [93], with time (POST vs PRE) as the main fixed effect, the same baseline covariates, a subject-level random intercept, and Benjamini–Hochberg FDR correction applied across genera within each specimen.

4.11. Multi-Omics Data Integration

Multi-omics integration was performed using Multi-Omics Factor Analysis (MOFA) [94]. The model included the following data layers (views): salivary and serum cytokines (CYT-S, CYT-Se), serum metabolites and lipoproteins (MET-Se, LIP-Se), salivary and fecal metabolomics (MET-S, MET-F), and microbiome genus-level profiles from saliva, lesional mucosa, non-lesional mucosa, and feces (16S-S, 16S-L, 16S-NL, 16S-F).

For each feature within each view, within-subject changes were computed as delta values (POST − PRE). To adjust for baseline covariates, feature-wise linear regression models were fitted with delta values as the response and age, sex, BMI, baseline vitamin D levels, and baseline disease severity as covariates; regression residuals were retained as covariate-adjusted change estimates for integration. Residuals were winsorized at the 1st and 99th percentiles within each feature to limit the influence of extreme values.

MOFA was trained on the covariate-adjusted, winsorized residual matrices using MOFA2 (v1.20.0) [94]. Model inference was initialized with a maximum of five latent factors (*num_factors = 5*), and factors explaining <5% of variance across all views were discarded during training (*drop_factor_threshold = 0.05*). Based on these settings, the final model retained three latent factors for downstream interpretation and visualization.

The fraction of variance explained was used to quantify the proportion of within-view variability captured by each latent factor. Feature-factor associations were evaluated using MOFA weights, retaining for visualization the top five features per view with $|\text{weight}| > 0.1$.

5. Conclusions

This study provides the first clinical evidence that combined probiotic and vitamin D supplementation can meaningfully improve the course of OLP. The integration of clinical, immunological, metabolomics and metagenomics data represents a key strength of our work, providing a multidimensional perspective on the potential mechanisms underlying the observed beneficial effects. The results suggest that this combined approach may improve OLP clinical course through a multifaceted mechanism, involving local modulation of mucosal inflammation, systemic metabolic benefits mediated by the gut-oral axis (including the production of indoles and antioxidant compounds), and favorable shifts in both oral and gut microbiota composition.

Despite their limitations, the methodology and data presented here could represent valuable support for future research and novel testable hypotheses. Larger, well-designed randomized controlled trials are warranted to confirm these observations and clarify the individual and combined effects of the interventions.

Supplementary Materials: The following supporting information can be downloaded at the website of this paper posted on Preprints.org. Additional material is provided as Supplementary File S1.

Author Contributions: Conceptualization, BA and PZ; Methodology, PZ, MC, M Mel, AV, M Mar, M Man, EB, VC, DFS and M All; Software, PZ, MC, M Mel, AV, M Man and EB; Validation, PZ, MC, M Mel, AV, M Man, EB and VC; Formal Analysis, PZ, MC, M Mel, AV, M Mar, M Man, EB, VC and M All; Investigation, PZ, MC, M Mel, AV, M Mar, M Man, EB, VC and M All; Resources, M Mel, AA, MP and BA; Data Curation, PZ, MC, M Mel, AV, M Mar, NV, LT, M Manf, EB, M Mig and M Arm; Writing-Original Draft Preparation, PZ, MC, AV and BA; Writing-Review and Editing, MC, M Mel, AV, M Mar, NV, LT, M Manf, EB, M Mig, M Arm, VC, AA, MP and BA; Visualization, PZ, MC, M Mel, AV, M Mar, M Man, EB, M Mig and M Arm; Supervision, LT, NV, M Mig

© 2026 by the author(s). Distributed under a Creative Commons CC BY license.

Preprints.org (www.preprints.org) | NOT PEER-REVIEWED | Posted: 22 May 2026 doi:10.20944/preprints202605.1565.v1

and BA; Project Administration, PZ, MC and BA; Funding Acquisition, LT and BA. All authors have read and agreed to the published version of the manuscript.

Funding: PZ: DFS and BA have been partially supported by Fondi di Ricerca di Ateneo (FAR-2017) provided by UPO. PZ has been supported by a competitive Scholarship for the PhD program in "Food, Health and Longevity" financed by the Ministry of Education, University and Research (MIUR, Italy). M Arm holds a PhD career grant supported by Next Generation EU - MUR (Italy) for the PhD program in Food, Health and Longevity Studies, XXXIX cycle. AV and LT acknowledge co-funding from Next Generation EU, in the context of the National Recovery and Resilience Plan, M4C2 Investment 1.3—Research Program PE8 Project Age-It: "Ageing Well in an Ageing Society" (CUP B83C22004800006). The APC was funded by Probiotical Research S.r.l.

Institutional Review Board Statement: This study protocol, conducted as a pilot clinical investigation, was approved by the Local Ethics Committee (Comitato Etico Interaziendale, CEI) of the Azienda Ospedaliero-Universitaria (AOU) Maggiore della Carità (Novara, Italy) serving as an Institutional Review Board (IRB) (Protocol Number 801/CE, Approval Study Number CE 143/21), in accordance with the ethical guidelines of the governmental agency and with the Declaration of Helsinki and its Edinburgh amendments.

Informed Consent Statement: All the patients were asked to carefully read and sign informed written consent. All participants provided written informed consent prior to inclusion in the study. The study was conducted in accordance with the Declaration of Helsinki.

Data Availability Statement: The dataset supporting the conclusions of this article is available in the "MICROCOSM in vivo study data" repository [https://doi.org/10.5281/zenodo.19188548].

Acknowledgments: We acknowledge the support of the Integrative Genomics Core Facility (CAAD, Università del Piemonte Orientale) and thank Marta Mellai and Marta Allesina for technical assistance. .We acknowledge the support of the Protein Technologies and Metabolism Core Facility (CAAD, Università del Piemonte Orientale) and thank Valeria Caneparo and Elia Amede for technical assistance. We would like to thank Santina Castriciano of Copan Italia S.p.A. for providing the e-NAT® swabs and sharing the experimental procedures to collect and manage patients' oral swabs. Vita D3 and the probiotic blend were provided by Erba Vita Group S.p.A. and Probiotical Research S.r.l., respectively. The authors have reviewed and edited the output and take full responsibility for the content of this publication.

Conflicts of Interest: The authors declare no conflicts of interest. AA and MP were employed by Probiotical Research S.r.l. They had no role in the design of the study; in the collection, analyses, or interpretation of data; in the writing of the manuscript; or in the decision to publish the results. All authors declare that the research was conducted in the absence of any commercial or financial relationships that could be construed as a potential conflict of interest.

© 2026 by the author(s). Distributed under a Creative Commons CC BY license.

Preprints.org (www.preprints.org) | NOT PEER-REVIEWED | Posted: 22 May 2026 doi:10.20944/preprints202605.1565.v1

Abbreviations

The following abbreviations are used in this manuscript:

OLP oral lichen planus	
NF-κB	nuclear factor-kappa B
MMPs	Matrix metalloproteinases
WHO	World Health Organization
OSCC	oral squamous cell carcinoma
Treg regulatory T cells	
Th17 T-helper 17	
IL interleukin	
TGF- β	Transforming Growth Factor-beta
CFSs Cell Free Supernatants	
Th1 T-helper 1	
IFN-γ	interferon-gamma
CEI Comitato Etico Interaziendale	
AOU	Azienda Ospedaliero-Universitaria
IRB Institutional Review Board	
LRE11	*Limosilactobacillus reuteri*
LR04 *Lacticasebacillus rhamnosus*	
LC04 *Lacticasebacillus casei*	
AFU	Active Fluorescent Units
CFU	Colony Forming Units
s	seconds
BMI	body mass index
SE	serum
S	saliva
L	OLP-lesioned mucosa
NL	non-lesioned healthy mucosa
F	feces
min minutes	
RT	room temperature
h	hours
sCD40L	soluble CD40 ligand
TNFα	tumor necrosis factor alpha
NMR	nuclear magnetic resonance
ATM	automatic tuning and matching
NOESY	nuclear Overhauser effect spectroscopy
MW molecular weight	
ACN acetonitrile	
IPA isopropanol	

© 2026 by the author(s). Distributed under a Creative Commons CC BY license.

Preprints.org (www.preprints.org) | NOT PEER-REVIEWED | Posted: 22 May 2026 doi:10.20944/preprints202605.1565.v1

RDP	Ribosomal Database Project
FDR false discovery rate	
CLR centered log-ratio	
PCoA	principal component analysis
MOFA	Multi-Omics Factor Analysis
CYT-S	salivary cytokines
CYT-Se	serum cytokines
MET-Se	serum metabolites
LIP	Seserum lipoproteins
MET-S	salivary metabolomics
MET-F	fecal metabolomics
16S-S	salivary microbiome
16S-L	lesional microbiome
16S-NL	non-lesional microbiome
16S-F	fecal microbiome
AIFA	Agenzia Italiana del Farmaco

References

1. González-Moles, M.Á.; Warnakulasuriya, S.; González-Ruiz, I.; González-Ruiz, L.; Ayén, Á.; Lenouvel, D.; Ruiz-Ávila, I.; Ramos-García, P. Worldwide Prevalence of Oral Lichen Planus: A Systematic Review and Meta-analysis. *Oral Diseases* **2021**, *27*, 813–828, doi:10.1111/odi.13323.
2. Liu, Y.; Messadi, D.; Wu, H.; Hu, S. Oral Lichen Planus Is a Unique Disease Model for Studying Chronic Inflammation and Oral Cancer. *Med Hypotheses* **2010**, *75*, 492–494, doi:10.1016/j.mehy.2010.07.002.
3. Idrees, M.; Kujan, O.; Shearston, K.; Farah, C.S. Oral Lichen Planus Has a Very Low Malignant Transformation Rate: A Systematic Review and Meta-Analysis Using Strict Diagnostic and Inclusion Criteria. *Journal of Oral Pathology & Medicine* **2021**, *50*, 287–298, doi:10.1111/jop.12996.
4. Ramos-García, P.; González-Moles, M.Á.; Warnakulasuriya, S. Oral Cancer Development in Lichen Planus and Related Conditions—3.0 Evidence Level: A Systematic Review of Systematic Reviews. *Oral Diseases* **2021**, *27*, 1919–1935, doi:10.1111/odi.13812.
5. Petruzzi, M.; della Vella, F.; Squicciarini, N.; Lilli, D.; Campus, G.; Piazzolla, G.; Lucchese, A.; Van Der Waal, I. Diagnostic Delay in Autoimmune Oral Diseases. *Oral Diseases* **2023**, *29*, 2614–2623, doi:10.1111/odi.14480.
6. Mutafchieva, M.Z.; Tashkova, D.A. Discrepancy in the Histological Diagnoses of Oral Lichen Planus Based on WHO Criteria Versus the Newly Proposed Diagnostic Set of the American Academy of Oral and Maxillofacial Pathology. *Diagnostics* **2025**, *15*, 558, doi:10.3390/diagnostics15050558.
7. Gururaj, N.; Hasinidevi, P.; Janani, V.; Divynadaniel, T. Diagnosis and Management of Oral Lichen Planus - Review. *J Oral Maxillofac Pathol* **2021**, *25*, 383–393, doi:10.4103/jomfp.jomfp_386_21.
8. Nielsen, F.; Mikkelsen, B.B.; Nielsen, J.B.; Andersen, H.R.; Grandjean, P. Plasma Malondialdehyde as Biomarker for Oxidative Stress: Reference Interval and Effects of Life-Style Factors. *Clin Chem* **1997**, *43*, 1209–1214.
9. Torrente-Castells, E.; Figueiredo, R.; Berini-Aytes, L.; Gay-Escoda, C. Clinical Features of Oral Lichen Planus. A Retrospective Study of 65 Cases. *Med Oral* **2010**, e685–e690, doi:10.4317/medoral.15.e685.
10. Bombeccari, G.P.; Guzzi, G.; Tettamanti, M.; Giannì, A.B.; Baj, A.; Pallotti, F.; Spadari, F. Oral Lichen Planus and Malignant Transformation: A Longitudinal Cohort Study. *Oral Surgery, Oral Medicine, Oral Pathology, Oral Radiology, and Endodontology* **2011**, *112*, 328–334, doi:10.1016/j.tripleo.2011.04.009.
11. Bui, F.Q.; Almeida-da-Silva, C.L.C.; Huynh, B.; Trinh, A.; Liu, J.; Woodward, J.; Asadi, H.; Ojcius, D.M. Association between Periodontal Pathogens and Systemic Disease. *Biomedical Journal* **2019**, *42*, 27–35, doi:10.1016/j.bj.2018.12.001.
12. Tuominen, H.; Rautava, J. Oral Microbiota and Cancer Development. *Pathobiology* **2021**, *88*, 116–126, doi:10.1159/000510979.

© 2026 by the author(s). Distributed under a Creative Commons CC BY license.

Preprints.org (www.preprints.org) | NOT PEER-REVIEWED | Posted: 22 May 2026 doi:10.20944/preprints202605.1565.v1

13. Cheng, Y.-S.L.; Gould, A.; Kurago, Z.; Fantasia, J.; Muller, S. Diagnosis of Oral Lichen Planus: A Position Paper of the American Academy of Oral and Maxillofacial Pathology. *Oral Surgery, Oral Medicine, Oral Pathology and Oral Radiology* **2016**, *122*, 332–354, doi:10.1016/j.oooo.2016.05.004.
14. Han, X.; Zhang, J.; Tan, Y.; Zhou, G. Probiotics: A Non-Conventional Therapy for Oral Lichen Planus. *Archives of Oral Biology* **2017**, *81*, 90–96, doi:10.1016/j.archoralbio.2017.04.026.
15. Roopashree, M.R.; Gondhalekar, R.V.; Shashikanth, M.C.; George, J.; Thippeswamy, S.H.; Shukla, A. Pathogenesis of Oral Lichen Planus - a Review: Pathogenesis of Oral Lichen Planus. *Journal of Oral Pathology & Medicine* **2010**, *39*, 729–734, doi:10.1111/j.1600-0714.2010.00946.x.
16. Daume, L.; Kreis, C.; Bohner, L.; Kleinheinz, J.; Jung, S. Does the Clinical Form of Oral Lichen Planus (OLP) Influence the Oral Health–Related Quality of Life (OHRQoL)? *IJERPH* **2020**, *17*, 6633, doi:10.3390/ijerph17186633.
17. Barnes, E.L.; Eveson, J.W.; Reichart, P.; Sidransky, D. Pathology & Genetics Head and Neck Tumours.
18. Gonzalez-Moles, M.; Scully, C.; Gil-Montoya, J. Oral Lichen Planus: Controversies Surrounding Malignant Transformation. *Oral Diseases* **2008**, *14*, 229–243, doi:10.1111/j.1601-0825.2008.01441.x.
19. Ślebioda, Z.; Drożdżyńska, J.; Karpińska, A.; Krzyżaniak, A.; Kasperczak, M.; Tomoń, N.; Wiśniewska, P.; Wyganowska, M.L. Oral Lichen Planus: Clinical Presentation, Demographic Characteristics, and Risk Factors in a Retrospective Study of 186 Polish Patients. *JCM* **2024**, *13*, 7363, doi:10.3390/jcm13237363.
20. Hallopeau, H. Sur Un Cas de Lichen de Wilson Gingival Avec Neoplastic Voisine Dans La Region Maxillaire. *Bull Soc Fr Dermatol Syphiligr* **1910**.
21. Li, Y.; Shao, F.; Zheng, S.; Tan, Z.; He, Y. Alteration of Streptococcus Salivarius in Buccal Mucosa of Oral Lichen Planus and Controlled Clinical Trial in OLP Treatment. *Probiotics & Antimicro. Prot.* **2020**, *12*, 1340–1348, doi:10.1007/s12602-020-09664-5.
22. Petruzzi, M.; Lucchese, A.; Lajolo, C.; Campus, G.; Lauritano, D.; Serpico, R. Topical Retinoids in Oral Lichen Planus Treatment: An Overview. *Dermatology* **2013**, *226*, 61–67, doi:10.1159/000346750.
23. Malik, U.; Gupta, S.; Malik, S.D.; Vashishth, S.; Zaheeruddin; Raju, M.S. Treatment of Symptomatic Oral Lichen Planus (OLP) with 0.1% Tacrolimus Powder in Oraguard-B – A Pilot Prospective Study. *The Saudi Dental Journal* **2012**, *24*, 143–148, doi:10.1016/j.sdentj.2012.05.002.
24. Yokomizo, S.; Kaneko, N.; Chen, H.; Yan, L.; Tsuji, S.; Akagawa, S.; Sameshima, J.; Sueyoshi, T.; Nagano, H.; Miyahara, Y.; et al. Dysbiosis of the Gut Microbiome May Contribute to the Pathogenesis of Oral Lichen Planus through Treg Dysregulation. *Mucosal Immunology* **2025**, *18*, 1013–1026, doi:10.1016/j.mucimm.2025.05.009.
25. Chowdhury, A.H.; Cámara, M.; Verma, C.; Eremin, O.; Kulkarni, A.D.; Lobo, D.N. Modulation of T Regulatory and Dendritic Cell Phenotypes Following Ingestion of Bifidobacterium Longum, AHCC® and Azithromycin in Healthy Individuals. *Nutrients* **2019**, *11*, 2470, doi:10.3390/nu11102470.
26. Fan, Z.; Ross, R.P.; Stanton, C.; Hou, B.; Zhao, J.; Zhang, H.; Yang, B.; Chen, W. Lactobacillus Casei CCFM1074 Alleviates Collagen-Induced Arthritis in Rats via Balancing Treg/Th17 and Modulating the Metabolites and Gut Microbiota. *Front. Immunol.* **2021**, *12*, 680073, doi:10.3389/fimmu.2021.680073.
27. Khorasani, S.; Mahmoudi, M.; Kalantari, M.R.; Lavi Arab, F.; Esmaeili, S.; Mardani, F.; Tabasi, N.; Rastin, M. Amelioration of Regulatory T Cells by *Lactobacillus Delbrueckii* and *Lactobacillus Rhamnosus* in Pristane-induced Lupus Mice Model. *Journal Cellular Physiology* **2019**, *234*, 9778–9786, doi:10.1002/jcp.27663.
28. Zanetta, P.; De Giorgis, V.; Barberis, E.; Manfredi, M.; Amoruso, A.; Pane, M.; Azzimonti, B. Lactobacillus Probiotic Cell-Free Supernatants and Vitamin D Influence Interleukin-6 Production and Mitigate Oral Periodontopathogens-Induced Cytotoxicity in FaDu Cells. *Front. Microbiol.* **2025**, *16*, 1578267, doi:10.3389/fmicb.2025.1578267.
29. Kwon, H.-K.; Lee, C.-G.; So, J.-S.; Chae, C.-S.; Hwang, J.-S.; Sahoo, A.; Nam, J.H.; Rhee, J.H.; Hwang, K.-C.; Im, S.-H. Generation of Regulatory Dendritic Cells and $CD4^+$ $Foxp3^+$ T Cells by Probiotics Administration Suppresses Immune Disorders. *Proc. Natl. Acad. Sci. U.S.A.* **2010**, *107*, 2159–2164, doi:10.1073/pnas.0904055107.
30. Ren, S.; Zhang, X.; Guan, H.; Wu, L.; Yu, M.; Hou, D.; Yan, Y.; Fang, X. Lactobacillus Acidipiscis Induced Regulatory Gamma Delta T Cells and Attenuated Experimental Autoimmune Encephalomyelitis. *Front. Immunol.* **2021**, *12*, 623451, doi:10.3389/fimmu.2021.623451.

© 2026 by the author(s). Distributed under a Creative Commons CC BY license.

Preprints.org (www.preprints.org) | NOT PEER-REVIEWED | Posted: 22 May 2026 doi:10.20944/preprints202605.1565.v1

31. Paria Motahari; Fatemeh Pournaghi Azar; Arefeh Rasi Role of Vitamin D and Vitamin D Receptor in Oral Lichen Planus: A Systematic Review. *Ethiop J Health Sci* **2020**, *30*, doi:10.4314/ejhs.v30i4.17.
32. Shalaby, R.; Nabil, G.; Ibrahim, S.; Kotb, A.A.; Amer, H.; Afifi, S. The Role of Vitamin D Deficiency in the Development and Severity of Oral Lichen Planus: A Case-Control Study. *Clin Oral Invest* **2025**, *29*, 320, doi:10.1007/s00784-025-06398-y.
33. Kumar, R.; Sood, U.; Gupta, V.; Singh, M.; Scaria, J.; Lal, R. Recent Advancements in the Development of Modern Probiotics for Restoring Human Gut Microbiome Dysbiosis. *Indian J Microbiol* **2020**, *60*, 12–25, doi:10.1007/s12088-019-00808-y.
34. Singh, P.; Rawat, A.; Alwakeel, M.; Sharif, E.; Al Khodor, S. The Potential Role of Vitamin D Supplementation as a Gut Microbiota Modifier in Healthy Individuals. *Sci Rep* **2020**, *10*, 21641, doi:10.1038/s41598-020-77806-4.
35. Shalaby, R.; Nawawy, M.E.; Selim, K.; Bahaa, S.; Refai, S.E.; Maksoud, A.E.; Sayed, M.E.; Essawy, A.; Elshaer, A.; ElShaer, M.; et al. The Role of Vitamin D in Amelioration of Oral Lichen Planus and Its Effect on Salivary and Tissue IFN-γ Level: A Randomized Clinical Trial. *BMC Oral Health* **2024**, *24*, 813, doi:10.1186/s12903-024-04239-0.
36. Rahmadhini, E.; Hidayat, W.; Zakiawati, D. Vitamin D in the Treatment of Recalcitrant Oral Lichen Planus: A Case Series. *IJWH* **2025**, *Volume 17*, 3229–3239, doi:10.2147/IJWH.S527877.
37. Keller, M.; Kragelund, C. Randomized Pilot Study on Probiotic Effects on Recurrent Candidiasis in Oral Lichen Planus Patients. *Oral Diseases* **2018**, *24*, 1107–1114, doi:10.1111/odi.12858.
38. Marlina, E.; Goodman, R.N.; Mercadante, V.; Shephard, M.; McMillan, R.; Hodgson, T.; Leeson, R.; Porter, S.; Barber, J.A.; Fedele, S.; et al. A Proof of Concept Pilot Trial of Probiotics in Symptomatic Oral Lichen Planus (CABRIO). *Oral Diseases* **2022**, *28*, 2155–2167, doi:10.1111/odi.14014.
39. Abboud, M.; Rizk, R.; AlAnouti, F.; Papandreou, D.; Haidar, S.; Mahboub, N. The Health Effects of Vitamin D and Probiotic Co-Supplementation: A Systematic Review of Randomized Controlled Trials. *Nutrients* **2020**, *13*, 111, doi:10.3390/nu13010111.
40. Lopez, J.; Ramos-Plaza, V.; Rodriguez-Morales, B.M.; Cruz, M.L.; Appleyard, C.B. Exploring the Synergistic Potential of Probiotics and Vitamin D to Ameliorate Acute TNBS-Induced Colitis in Mice. *Physiology* **2024**, *39*, 961, doi:10.1152/physiol.2024.39.S1.961.
41. Zanetta, P.; Squarzanti, D.F.; Di Coste, A.; Rolla, R.; Valletti, P.A.; Garzaro, M.; Dell'Era, V.; Amoruso, A.; Pane, M.; Azzimonti, B. In Vitro Selection of Lactobacillus and Bifidobacterium Probiotic Strains for the Management of Oral Pathobiont Infections Associated to Systemic Diseases. *IJMS* **2022**, *23*, 16163, doi:10.3390/ijms232416163.
42. AghaHosseini, F.; Tahmasebinasab, M.; Vatanpour, M. Exploring the Link Between Oral Lichen Planus and Xerostomia: A Systematic Literature Review. *Immun Inflamm Dis* **2024**, *12*, e70101, doi:10.1002/iid3.70101.
43. Družijanić, A.; Cigić, L.; Glavina, A.; Draganja, M.; Martinović, D.; Ković, M. Serum Concentration of Vitamin D in Patients with Oral Lichen Planus. *Acta Stomatol Croat* **2023**, *57*, 265–272, doi:10.15644/asc57/3/7.
44. Nigam, K.; Singh, N.; Yadav, S.K.; Sanyal, S. The Taq 1 Polymorphism of Vitamin D Receptor Gene Is Associated with Oral Cancer and Preoral Cancer in North Indian Population. *Journal of Cancer Research and Therapeutics* **2023**, *19*, 403–407, doi:10.4103/jcrt.jcrt_109_22.
45. Saeed, S.; Choudhury, P.; Ahmad, S.A.; Alam, T.; Panigrahi, R.; Aziz, S.; Kaleem, S.M.; Priyadarshini, S.R.; Sahoo, P.K.; Hasan, S. Vitamin D in the Treatment of Oral Lichen Planus: A Systematic Review. *Biomedicines* **2022**, *10*, 2964, doi:10.3390/biomedicines10112964.
46. Marssafy Lama H.; Fatma Hussein; Hesham Sadek; Wahdan Abdelghany Serum Vitamin D Level in Healthy Individuals versus Patients with Symptomatic Andasymptomatic Oral Lichen Planus. *Cell Mol Biol (Noisy-le-grand)* **2022**, *68*, 19–25, doi:10.14715/cmb/2022.68.2.3.
47. Afzali, S.; Mohammadisoleimani, E.; Mansoori, Y.; Mohaghegh, P.; Bahmanyar, M.; Mansoori, B.; Pezeshki, B.; Nikfar, G.; Tavassoli, A.; Shahi, A.; et al. The Potential Roles of Th17 Cells in the Pathogenesis of Oral Lichen Planus. *Inflamm. Res.* **2023**, *72*, 1513–1524, doi:10.1007/s00011-023-01763-7.
48. Duchesne, M.; Okoye, I.; Lacy, P. Epithelial Cell Alarmin Cytokines: Frontline Mediators of the Asthma Inflammatory Response. *Front. Immunol.* **2022**, *13*, 975914, doi:10.3389/fimmu.2022.975914.

© 2026 by the author(s). Distributed under a Creative Commons CC BY license.

Preprints.org (www.preprints.org) | NOT PEER-REVIEWED | Posted: 22 May 2026 doi:10.20944/preprints202605.1565.v1

49. García-Roza, P.; García-Pola, M. Inflammatory Markers and Dyslipidemia in Patients with Oral Lichen Planus: A Case–Control Study. *Diagnostics* **2025**, *15*, 2783, doi:10.3390/diagnostics15212783.
50. Lai, Y.C.; Yew, Y.W.; Schwartz, R.A. Lichen Planus and Dyslipidemia: A Systematic Review and Meta-analysis of Observational Studies. *Int J Dermatology* **2016**, *55*, doi:10.1111/ijd.13234.
51. Wang, C.; Li, S.; Xue, P.; Yu, L.; Tian, F.; Zhao, J.; Chen, W.; Xue, Y.; Zhai, Q. The Effect of Probiotic Supplementation on Lipid Profiles in Adults with Overweight or Obesity: A Meta-Analysis of Randomized Controlled Trials. *Journal of Functional Foods* **2021**, *86*, 104711, doi:10.1016/j.jff.2021.104711.
52. Radkhah, N.; Zarezadeh, M.; Jamilian, P.; Ostadrahimi, A. The Effect of Vitamin D Supplementation on Lipid Profiles: An Umbrella Review of Meta-Analyses. *Advances in Nutrition* **2023**, *14*, 1479–1498, doi:10.1016/j.advnut.2023.08.012.
53. Dibaba, D.T. Effect of Vitamin D Supplementation on Serum Lipid Profiles: A Systematic Review and Meta-Analysis. *Nutr Rev* **2019**, *77*, 890–902, doi:10.1093/nutrit/nuz037.
54. Xu, Q.; Wang, W.; Li, Y.; Cui, J.; Zhu, M.; Liu, Y.; Liu, Y. The Oral-Gut Microbiota Axis: A Link in Cardiometabolic Diseases. *npj Biofilms Microbiomes* **2025**, *11*, 11, doi:10.1038/s41522-025-00646-5.
55. Faure, M.; Moënnoz, D.; Montigon, F.; Mettraux, C.; Breuillé, D.; Ballèvre, O. Dietary Threonine Restriction Specifically Reduces Intestinal Mucin Synthesis in Rats. *The Journal of Nutrition* **2005**, *135*, 486–491, doi:10.1093/jn/135.3.486.
56. Scott, S.A.; Fu, J.; Chang, P.V. Microbial Tryptophan Metabolites Regulate Gut Barrier Function via the Aryl Hydrocarbon Receptor. *Proc. Natl. Acad. Sci. U.S.A.* **2020**, *117*, 19376–19387, doi:10.1073/pnas.2000047117.
57. Youm, Y.-H.; Nguyen, K.Y.; Grant, R.W.; Goldberg, E.L.; Bodogai, M.; Kim, D.; D'Agostino, D.; Planavsky, N.; Lupfer, C.; Kanneganti, T.D.; et al. The Ketone Metabolite β-Hydroxybutyrate Blocks NLRP3 Inflammasome–Mediated Inflammatory Disease. *Nat Med* **2015**, *21*, 263–269, doi:10.1038/nm.3804.
58. Manandhar, M.; Cronan, J.E. Pimelic Acid, the First Precursor of the Bacillus Subtilis Biotin Synthesis Pathway, Exists as the Free Acid and Is Assembled by Fatty Acid Synthesis. *Molecular Microbiology* **2017**, *104*, 595–607, doi:10.1111/mmi.13648.
59. Ren, Z.; Xu, Y.; Li, T.; Sun, W.; Tang, Z.; Wang, Y.; Zhou, K.; Li, J.; Ding, Q.; Liang, K.; et al. NAD+ and Its Possible Role in Gut Microbiota: Insights on the Mechanisms by Which Gut Microbes Influence Host Metabolism. *Animal Nutrition* **2022**, *10*, 360–371, doi:10.1016/j.aninu.2022.06.009.
60. Niño-Narvión, J.; Rojo-López, M.I.; Martinez-Santos, P.; Rossell, J.; Ruiz-Alcaraz, A.J.; Alonso, N.; Ramos-Molina, B.; Mauricio, D.; Julve, J. NAD+ Precursors and Intestinal Inflammation: Therapeutic Insights Involving Gut Microbiota. *Nutrients* **2023**, *15*, doi:10.3390/nu15132992.
61. Qi, Y.; Zang, S.; Wei, J.; Yu, H.; Yang, Z.; Wu, H.; Kang, Y.; Tao, H.; Yang, M.; Jin, L.; et al. High-Throughput Sequencing Provides Insights into Oral Microbiota Dysbiosis in Association with Inflammatory Bowel Disease. *Genomics* **2021**, *113*, 664–676, doi:10.1016/j.ygeno.2020.09.063.
62. Sanadi, R.M.; Khandekar, P.D.; Chaudhari, S.R.; Javali, M.A.; Gurav, N.U. Association of Periodontal Disease with Oral Lichen Planus: A Systematic Review and Meta Analysis. *J Oral Maxillofac Pathol* **2023**, *27*, 173–180, doi:10.4103/jomfp.jomfp_178_22.
63. Routier, A.; Blaizot, A.; Agossa, K.; Dubar, M. What Do We Know about the Mechanisms of Action of Probiotics on Factors Involved in the Pathogenesis of Periodontitis? A Scoping Review of *in Vitro* Studies. *Archives of Oral Biology* **2021**, *129*, 105196, doi:10.1016/j.archoralbio.2021.105196.
64. Donati, C.; Zolfo, M.; Albanese, D.; Tin Truong, D.; Asnicar, F.; Iebba, V.; Cavalieri, D.; Jousson, O.; De Filippo, C.; Huttenhower, C.; et al. Uncovering Oral Neisseria Tropism and Persistence Using Metagenomic Sequencing. *Nat Microbiol* **2016**, *1*, 16070, doi:10.1038/nmicrobiol.2016.70.
65. Sragi, Z.; Vasan, V.; Laitman, B.M.; Rivera-Rivera, G.; Powers, A.; Dickstein, D.R.; Kirke, D.N.; Courey, M.S. Microbial Composition of the Laryngotracheal Region: A Systematic Review. *The Laryngoscope* **2024**, *134*, 4167–4175, doi:10.1002/lary.31453.
66. Ju, H.-M.; Ahn, Y.-W.; Ok, S.-M.; Jeong, S.-H.; Na, H.-S.; Chung, J. Microbial Profiles in Oral Lichen Planus: Comparisons with Healthy Controls and Erosive vs. Non-Erosive Subtypes. *Diagnostics* **2024**, *14*, 828, doi:10.3390/diagnostics14080828.
67. Thompson, J.; Pikis, A. Metabolism of Sugars by Genetically Diverse Species of Oral Leptotrichia. *Molecular Oral Microbiology* **2012**, *27*, 34–44, doi:10.1111/j.2041-1014.2011.00627.x.

© 2026 by the author(s). Distributed under a Creative Commons CC BY license.

Preprints.org (www.preprints.org) | NOT PEER-REVIEWED | Posted: 22 May 2026 doi:10.20944/preprints202605.1565.v1

68. Collado, L.; Figueras, M.J. Taxonomy, Epidemiology, and Clinical Relevance of the Genus Arcobacter. *Clinical Microbiology Reviews* **2011**, *24*, 174–192, doi:10.1128/cmr.00034-10.
69. Erira, A.; García Robayo, D.A.; Chalá, A.I.; Moreno Torres, A.; Muñoz Lopez, E.E.; Cid Arregui, A.; Tobar Tosse, F.; Gamboa Jaimes, F.O. Bacteriome Identified by Next-Generation Sequencing in Saliva, Dental Plaque, and Tumor Tissue of Patients with Oral Squamous Cell Carcinoma. **2021**, doi:10.2174/1874285802115010098.
70. Limo, L.; Donovan, J.; Frisbee, S.; Gomaa, N. The Exposome and the Human Oral Microbiome through the One Health Lens. *Archives of Oral Biology* **2026**, *183*, 106504, doi:10.1016/j.archoralbio.2026.106504.
71. Dahlen, G.; Basic, A.; Bylund, J. Importance of Virulence Factors for the Persistence of Oral Bacteria in the Inflamed Gingival Crevice and in the Pathogenesis of Periodontal Disease. *J Clin Med* **2019**, *8*, 1339, doi:10.3390/jcm8091339.
72. Jung, W.; Jang, S. Oral Microbiome Research on Oral Lichen Planus: Current Findings and Perspectives. *Biology* **2022**, *11*, 723, doi:10.3390/biology11050723.
73. He, Y.; Gong, D.; Shi, C.; Shao, F.; Shi, J.; Fei, J. Dysbiosis of Oral Buccal Mucosa Microbiota in Patients with Oral Lichen Planus. *Oral Diseases* **2017**, *23*, 674–682, doi:10.1111/odi.12657.
74. Zanetta, P.; Ormelli, M.; Amoruso, A.; Pane, M.; Azzimonti, B.; Squarzanti, D.F. Probiotics as Potential Biological Immunomodulators in the Management of Oral Lichen Planus: What's New? *IJMS* **2022**, *23*, 3489, doi:10.3390/ijms23073489.
75. Zhou, Q.; Liu, P.; Chen, M.; He, H.; Xu, M.; Xu, Q.; Yu, J.; Deng, Y.; Yan, J.; Wen, Y. Microbiological Mechanisms of Oral Mucosal Disease: Oral-Intestinal Crosstalk and Probiotic Therapy. *Front. Oral Health* **2025**, *6*, 1485028, doi:10.3389/froh.2025.1485028.
76. Gibson, M.K.; Pesesky, M.W.; Dantas, G. The Yin and Yang of Bacterial Resilience in the Human Gut Microbiota. *Journal of Molecular Biology* **2014**, *426*, 3866–3876, doi:10.1016/j.jmb.2014.05.029.
77. Bang, W.Y.; Moon, J.S.; Kim, H.; Lee, H.B.; Kim, D.; Shin, M.; Jung, Y.H.; Shin, J.; Yang, J. Therapeutic Modulation of the Gut Microbiome by Supplementation with Probiotics (SCI Microbiome Mix) in Adults with Functional Bowel Disorders: A Randomized, Double-Blind, Placebo-Controlled Trial. *Microorganisms* **2025**, *13*, 2283, doi:10.3390/microorganisms13102283.
78. Schütz, B.; Krause, F.F.; Taudte, R.V.; Zaiss, M.M.; Luu, M.; Visekruna, A. Modulation of Host Immunity by Microbiome-Derived Indole-3-Propionic Acid and Other Bacterial Metabolites. *Eur J Immunol* **2025**, *55*, e202451594, doi:10.1002/eji.202451594.
79. Rodríguez-Daza, M.C.; Pulido-Mateos, E.C.; Lupien-Meilleur, J.; Guyonnet, D.; Desjardins, Y.; Roy, D. Polyphenol-Mediated Gut Microbiota Modulation: Toward Prebiotics and Further. *Front. Nutr.* **2021**, *8*, 689456, doi:10.3389/fnut.2021.689456.
80. Wang, P.; Wang, R.; Zhao, W.; Zhao, Y.; Wang, D.; Zhao, S.; Ge, Z.; Ma, Y.; Zhao, X. Gut Microbiota-Derived 4-Hydroxyphenylacetic Acid from Resveratrol Supplementation Prevents Obesity through SIRT1 Signaling Activation. *Gut Microbes* **2025**, *17*, 2446391, doi:10.1080/19490976.2024.2446391.
81. World Medical Association World Medical Association Declaration of Helsinki: Ethical Principles for Medical Research Involving Human Participants. *JAMA* **2025**, *333*, 71–74, doi:10.1001/jama.2024.21972.
82. Vignoli, A.; Ghini, V.; Meoni, G.; Licari, C.; Takis, P.G.; Tenori, L.; Turano, P.; Luchinat, C. High-Throughput Metabolomics by 1D NMR. *Angew Chem Int Ed Engl* **2019**, *58*, 968–994, doi:10.1002/anie.201804736.
83. *ISO 23118:2021 Molecular in Vitro Diagnostic Examinations — Specifications for Pre-Examination Processes in Metabolomics in Urine, Venous Blood Serum and Plasma.*;
84. Bruzzone, C.; Bizkarguenaga, M.; Gil-Redondo, R.; Diercks, T.; Arana, E.; García De Vicuña, A.; Seco, M.; Bosch, A.; Palazón, A.; San Juan, I.; et al. SARS-CoV-2 Infection Dysregulates the Metabolomic and Lipidomic Profiles of Serum. *iScience* **2020**, *23*, 101645, doi:10.1016/j.isci.2020.101645.
85. Ghini, V.; Meoni, G.; Vignoli, A.; Di Cesare, F.; Tenori, L.; Turano, P.; Luchinat, C. Fingerprinting and Profiling in Metabolomics of Biosamples. *Progress in Nuclear Magnetic Resonance Spectroscopy* **2023**, *138–139*, 105–135, doi:10.1016/j.pnmrs.2023.10.002.
86. Jiménez, B.; Holmes, E.; Heude, C.; Tolson, R.F.; Harvey, N.; Lodge, S.L.; Chetwynd, A.J.; Cannet, C.; Fang, F.; Pearce, J.T.M.; et al. Quantitative Lipoprotein Subclass and Low Molecular Weight Metabolite Analysis

© 2026 by the author(s). Distributed under a Creative Commons CC BY license.

Preprints.org (www.preprints.org) | NOT PEER-REVIEWED | Posted: 22 May 2026 doi:10.20944/preprints202605.1565.v1

in Human Serum and Plasma by^{1} H NMR Spectroscopy in a Multilaboratory Trial. *Anal. Chem.* **2018**, *90*, 11962–11971, doi:10.1021/acs.analchem.8b02412.

87. Barberis, E.; Amede, E.; Tavecchia, M.; Marengo, E.; Cittone, M.G.; Rizzi, E.; Pedrinelli, A.R.; Tonello, S.; Minisini, R.; Pirisi, M.; et al. Understanding Protection from SARS-CoV-2 Using Metabolomics. *Sci Rep* **2021**, *11*, 13796, doi:10.1038/s41598-021-93260-2.
88. Ewing, B.; Hillier, L.; Wendl, M.C.; Green, P. Base-Calling of Automated Sequencer Traces Using *Phred*. I. Accuracy Assessment. *Genome Res.* **1998**, *8*, 175–185, doi:10.1101/gr.8.3.175.
89. Cole, S.W. Human Social Genomics. *PLoS Genet* **2014**, *10*, e1004601, doi:10.1371/journal.pgen.1004601.
90. Bates, D.; Mächler, M.; Bolker, B.; Walker, S. Fitting Linear Mixed-Effects Models Using **Lme4**. *J. Stat. Soft.* **2015**, *67*, doi:10.18637/jss.v067.i01.
91. Borman, T.; Ernst, F.G.M.; Shetty, S.A.; Lathi, L. Mia: Microbiome Analysis 2025.
92. Oksanen, J.; Simpson, G.L.; Blanchet, F.G.; Kindt, R.; Legendre, P.; Minchin, P.R.; O'Hara, R.B.; Solymos, P.; Stevens, M.H.H.; Szoecs, E.; et al. Vegan: Community Ecology Package 2001, 2.7-3.
93. Brooks, M., E.; Kristensen, K.; Benthem, K., J. ,van; Magnusson, A.; Berg, C., W.; Nielsen, A.; Skaug, H., J.; Mächler, M.; Bolker, B., M. glmmTMB Balances Speed and Flexibility Among Packages for Zero-Inflated Generalized Linear Mixed Modeling. *The R Journal* **2017**, *9*, 378, doi:10.32614/RJ-2017-066.
94. Argelaguet, R.; Velten, B.; Arnol, D.; Dietrich, S.; Zenz, T.; Marioni, J.C.; Buettner, F.; Huber, W.; Stegle, O. Multi-Omics Factor Analysis—a Framework for Unsupervised Integration of Multi-omics Data Sets. *Molecular Systems Biology* **2018**, *14*, e8124, doi:10.15252/msb.20178124.

Disclaimer/Publisher's Note: The statements, opinions and data contained in all publications are solely those of the individual author(s) and contributor(s) and not of MDPI and/or the editor(s). MDPI and/or the editor(s) disclaim responsibility for any injury to people or property resulting from any ideas, methods, instructions or products referred to in the content.

© 2026 by the author(s). Distributed under a Creative Commons CC BY license.